

Article

Pre-activated oxazaphosphorines designed for isophosphoramidate mustard delivery as bulk form or nano-assemblies: synthesis and proof of concept.

Charles Skarbek, Lea L. Lesueur, Hubert Chapuis, Alain Deroussent, Catherine Pioche-Durieu, Aurore Daville, Joachim Caron, Michael Rivard, Thierry Martens, Jean-Remi Bertrand, Eric Le Cam, Gilles Vassal, Patrick Couvreur, Didier Desmaële, and Angelo Paci

J. Med. Chem., **Just Accepted Manuscript** • DOI: 10.1021/jm501224x • Publication Date (Web): 11 Dec 2014

Downloaded from <http://pubs.acs.org> on December 21, 2014

Just Accepted

“Just Accepted” manuscripts have been peer-reviewed and accepted for publication. They are posted online prior to technical editing, formatting for publication and author proofing. The American Chemical Society provides “Just Accepted” as a free service to the research community to expedite the dissemination of scientific material as soon as possible after acceptance. “Just Accepted” manuscripts appear in full in PDF format accompanied by an HTML abstract. “Just Accepted” manuscripts have been fully peer reviewed, but should not be considered the official version of record. They are accessible to all readers and citable by the Digital Object Identifier (DOI®). “Just Accepted” is an optional service offered to authors. Therefore, the “Just Accepted” Web site may not include all articles that will be published in the journal. After a manuscript is technically edited and formatted, it will be removed from the “Just Accepted” Web site and published as an ASAP article. Note that technical editing may introduce minor changes to the manuscript text and/or graphics which could affect content, and all legal disclaimers and ethical guidelines that apply to the journal pertain. ACS cannot be held responsible for errors or consequences arising from the use of information contained in these “Just Accepted” manuscripts.



1
2
3
4
5
6
7
8
9
10
11
12
13
14
15
16
17
18
19
20
21
22
23
24
25
26
27
28
29
30
31
32
33
34
35
36
37
38
39
40
41
42
43
44
45
46
47
48
49
50
51
52
53
54
55
56
57
58
59
60

	Recherche Scientifique (CNRS), Laboratoire de Vectorologie et Thérapeutiques Anticancéreuses UMR 8203; Gustave Roussy Cancer Campus Grand Paris, Couvreur, Patrick; Université Paris-Sud, Institut Galien UMR 8612 Desmaële, Didier; Université Paris-Sud, Institut Galien UMR 8612 Paci, Angelo; Université Paris-Sud, Laboratoire de Vectorologie et Thérapeutiques Anticancéreuses UMR 8203; Centre National de la Recherche Scientifique (CNRS), Laboratoire de Vectorologie et Thérapeutiques Anticancéreuses UMR 8203; Gustave Roussy Cancer Campus Grand Paris, ; Gustave Roussy Cancer Campus Grand Paris, Service Interdépartemental de Pharmacologie et d'Analyse du Médicament

SCHOLARONE™
Manuscripts

1
2
3
4
5
6
7
8
9
10
11
12
13
14
15
16
17
18
19
20
21
22
23
24
25
26
27
28
29
30
31
32
33
34
35
36
37
38
39
40
41
42
43
44
45
46
47
48
49
50
51
52
53
54
55
56
57
58
59
60

Pre-activated oxazaphosphorines designed for isophosphoramidate mustard delivery as bulk form or nano-assemblies: synthesis and proof of concept.

Charles Skarbek^{1,2,3}, Lea L. Lesueur^{1,2,3}, Hubert Chapuis⁴, Alain Deroussent^{1,2,3}, Catherine Pioche-Durieu⁵, Aurore Daville^{1,2,3}, Joachim Caron⁴, Michael Rivard⁶, Thierry Martens⁶, Jean-Rémi Bertrand^{1,2,3}, Eric Le Cam⁵, Gilles Vassal^{1,2,3}, Patrick Couvreur⁴, Didier Desmaele⁴ and Angelo Paci^{1,2,3,7}.*

* Corresponding Author.

(1) Université Paris-Sud, Laboratoire de Vectorologie et Thérapeutiques Anticancéreuses, UMR 8203, Villejuif, France-94805;

(2) Centre National de la Recherche Scientifique (CNRS), Laboratoire de Vectorologie et Thérapeutiques Anticancéreuses, UMR 8203, Villejuif, France-94805;

(3) Gustave Roussy Cancer Campus Grand Paris, Laboratoire de Vectorologie et Thérapeutiques Anticancéreuses, UMR 8203, Villejuif, France-94805;

(4) Université Paris-Sud, Institut Galien, UMR 8612, Châtenay-Malabry, France-92296;

(5) CNRS UMR8126, Université Paris Sud 11, Institut Gustave Roussy, Villejuif, France-94805.

(6) Université Paris Est Créteil, Institut de Chimie et des Matériaux Paris-Est (ICMPE), UMR 7182, Thiais, France-94320;

1
2
3 **(7) Gustave Roussy Cancer Campus Grand Paris, Service Interdépartemental de**
4
5 **Pharmacologie et d'Analyse du Médicament (SIPAM), Villejuif, France-94805.**
6
7

8
9 KEYWORDS: Cancer, Cytotoxicity, Drug delivery; Ifosfamide, Nanomedicine, Nano-
10
11 assemblies, Oxazaphosphorines;.
12
13
14
15
16
17
18
19
20
21
22
23
24
25
26
27
28
29
30
31
32
33
34
35
36
37
38
39
40
41
42
43
44
45
46
47
48
49
50
51
52
53
54
55
56
57
58
59
60

1
2
3
4
5
6
7
8
9
10
11
12
13
14
15
16
17
18
19
20
21
22
23
24
25
26
27
28
29
30
31
32
33
34
35
36
37
38
39
40
41
42
43
44
45
46
47
48
49
50
51
52
53
54
55
56
57
58
59
60

ABSTRACT: Oxazaphosphorines are alkylating agents used in routine clinical practices for treatment of cancer for many years. They are antitumor prodrugs that require cytochrome P450 bio-activation leading to 4-hydroxy derivatives. In the case of ifosfamide (IFO), the bio-activation produces two toxic metabolites; acrolein, an urotoxic compound, concomitantly generated with the isophosphoramidate mustard and, chloroacetaldehyde, a neurotoxic and nephrotoxic compound, arising from the oxidation of the side chains. To improve the therapeutic index of IFO, we have designed pre-activated IFO derivatives with the covalent binding of several *O*- and *S*-alkyl moieties including poly-isoprenoid groups at the C-4 position of the oxazaphosphorine ring to avoid cytochrome bio-activation favoring the release of the active entity and limiting the chloroacetaldehyde release. Thanks to the grafted terpene moieties, some of these new conjugates demonstrated spontaneous self-assembling properties into nano-assemblies when dispersed in water. The cytotoxic activities on a panel of human tumor cell lines of these novel oxazaphosphorines, as bulk form or nano-assemblies, and the release of 4-hydroxy-IFO from these pre-activated IFO analogues in plasma are reported.

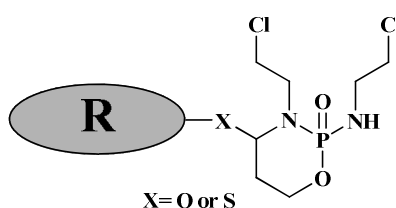
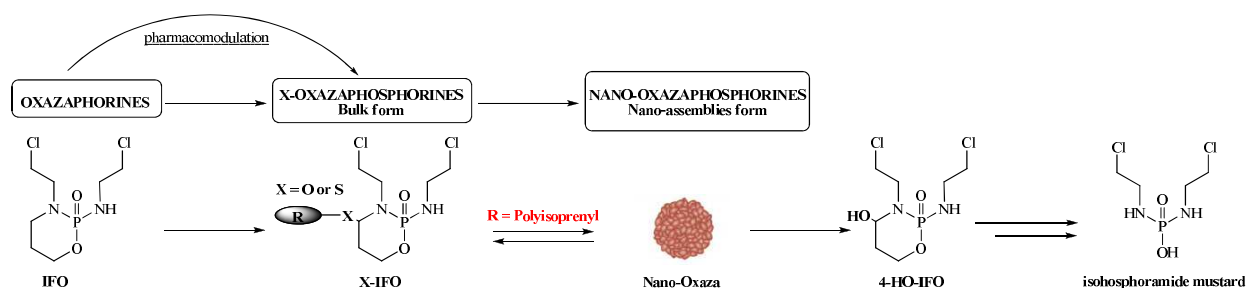
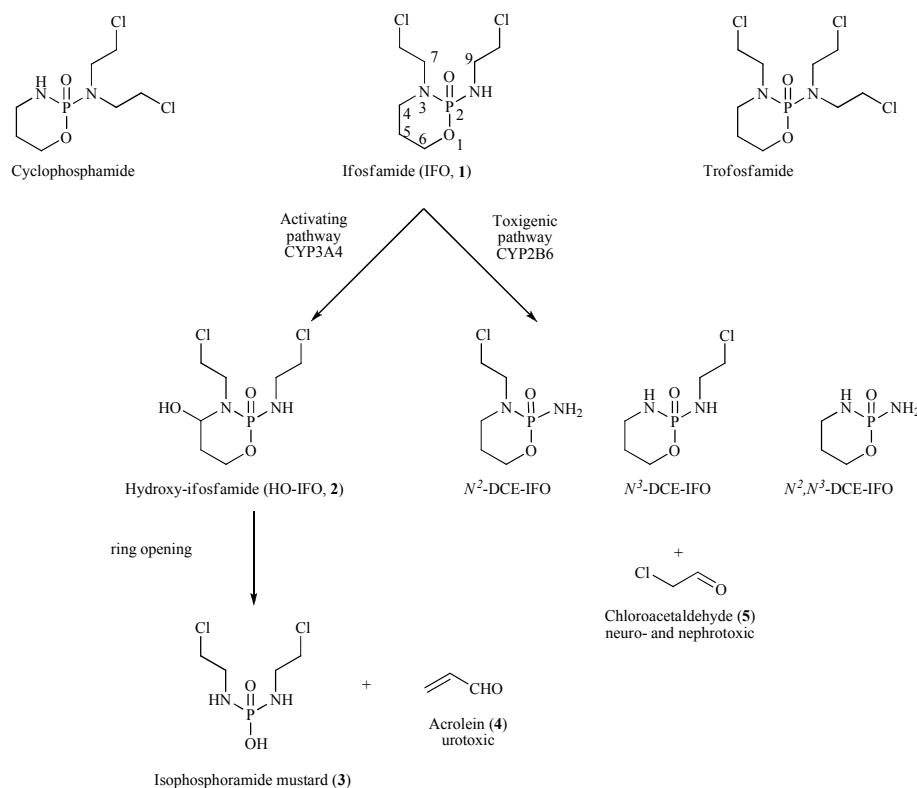


Table of contents graphic



1. Introduction.

Oxazaphosphorines belong to alkylating agents that have been widely used in routine clinical practices to treat several types of cancer from soft tissue tumor to lymphoma. Ifosfamide (IFO, **1**), cyclophosphamide and trofosfamide are oxazaphosphorines which contain two or three chloroethyl groups bounded to the nitrogen atoms (Scheme 1). As prodrugs, these compounds require a metabolic activation in position C-4 of the ring. This is fulfilled by specific liver cytochrome P450 (CYP)¹. In the case of IFO, this leads to a hydroxylated intermediate, the 4-hydroxy-ifosfamide (4-HO-IFO, **2**), which after a ring opening mechanism can release the active isophosphoramidate mustard (**3**) displaying cytotoxicity by DNA cross-links. This main activation pathway carried out by CYP3A4 leads concomitantly to the formation of acrolein (**4**) through tautomeric equilibrium and retro-Michael process. It is noteworthy that urotoxicity due to **4** and characterized by hemorrhagic cystitis, could be neutralized by co-administration of sodium mercaptoethanesulfonate (*mesna*).² A competitive CYP bio-activation of IFO by CYP2B6¹ (toxigenic pathway) occurring on the lateral chains (in positions C-7 and C-9) leads to the production of metabolites responsible for limiting side-effects. This secondary metabolism pathway, revealed during high dose protocols, oxidizes the chloroethyl side chains and leads to the release of *N*-deschloroethyl metabolites (*N*²-DCE-IFO, *N*³-DCE-IFO, *N*², *N*³-DCE-IFO) along with chloroacetaldehyde (**5**) responsible for neuro- and nephrotoxicity which remain not countered until today.

Scheme 1: Oxazaphosphorines and metabolism of Ifosfamide.

To circumvent the toxicity related to the release of chloroacetaldehyde, pharmacomodulation of IFO have been investigated. Synthesis of analogues by engraftment of methyl groups on the side chains (to avoid chloroacetaldehyde release)³ or replacement of the chlorine atoms by bromine⁴ was described. Agents⁵ that do not require *in vivo* biotransformation for activation including isophosphoramidate mustard^{6,7} and glufosfamide^{8,9} have also been proposed, some of them reaching phase I clinical trial such as mafosfamide¹⁰ or phase III for palifosfamide. Another strategy consists in the pre-activation of the oxazaphosphorine ring by chemical oxidation regioselectively centered on the C-4 position in order to bypass the cytochrome bio-activation. Many derivatives have already been prepared (4-OH,¹¹ 4-OOH,^{12,13} 4-OR, 4-SPh, 4-SCOR, 4-SCSR, 4-ONHCONH₂¹⁴). Although some of them showed improved *in vitro* activity, they were

1
2
3 found either too unstable for further development or with no advantages over the use of IFO even
4
5 so the concept of activation of the position C-4 was not shown to be a drawback and needs to be
6
7 pursued.
8
9

10 In this context, we assume that IFO analogues bearing long chain 4-alkoxy substituent might be
11
12 valuable candidates since steric hindrance around the *N*-3 nitrogen atom should slow down the
13
14 hydrolysis process to 4-HO-IFO and design more stable derivatives. However, the introduction
15
16 of simple alkoxy derivatives would dramatically reduce the water solubility. To address the
17
18 problem, we therefore chose to introduce various poly-isoprenoid chains at the C-4 position.
19
20 Indeed, we have previously shown that the covalent linkage of squalene, a natural triterpene
21
22 constituted of six isoprene units, to a drug belonging to various therapeutic classes, produced a
23
24 bioconjugate that self-assembled into nano-assemblies (NAs) in aqueous media¹⁵. In most cases,
25
26 the resulting NAs displayed an improved pharmaceutical profile compared to the parent
27
28 compound^{16,17,18,19}. The “squalenoylation” method, initially developed with highly hydrophilic
29
30 nucleoside analogues has been further extended to more hydrophobic drugs such as penicillin
31
32 G²⁰ or paclitaxel.²¹ Furthermore, we recently showed that other poly-isoprenoid compounds
33
34 derived from geraniol (2 isoprene units) and farnesol (3 isoprene units), were able to provide
35
36 self-assembling properties to the conjugates with nucleoside analogues.²² Based on these
37
38 findings, we hypothesize that the covalent binding of a poly-isoprenoid chain of a suitable size to
39
40 the C-4 carbon of IFO would deliver conjugates able to self-assemble into supramolecular
41
42 objects in aqueous media. In order to modulate the release of 4-HO-IFO, we decided to use
43
44 simple ether linker but also aminoethylsulfanyl linker. Thus, we report herein the synthesis of a
45
46 set of lipophilic derivatives of pre-activated IFO bearing, either a geranyl, a farnesyl, or a
47
48 squalene derived substituent at C-4 position (**9c-f**). To investigate the influence of the structural
49
50 features within the lipophilic side chain, IFO analogs bearing a simple alkyl group (**9a**) and
51
52
53
54
55
56
57
58
59
60

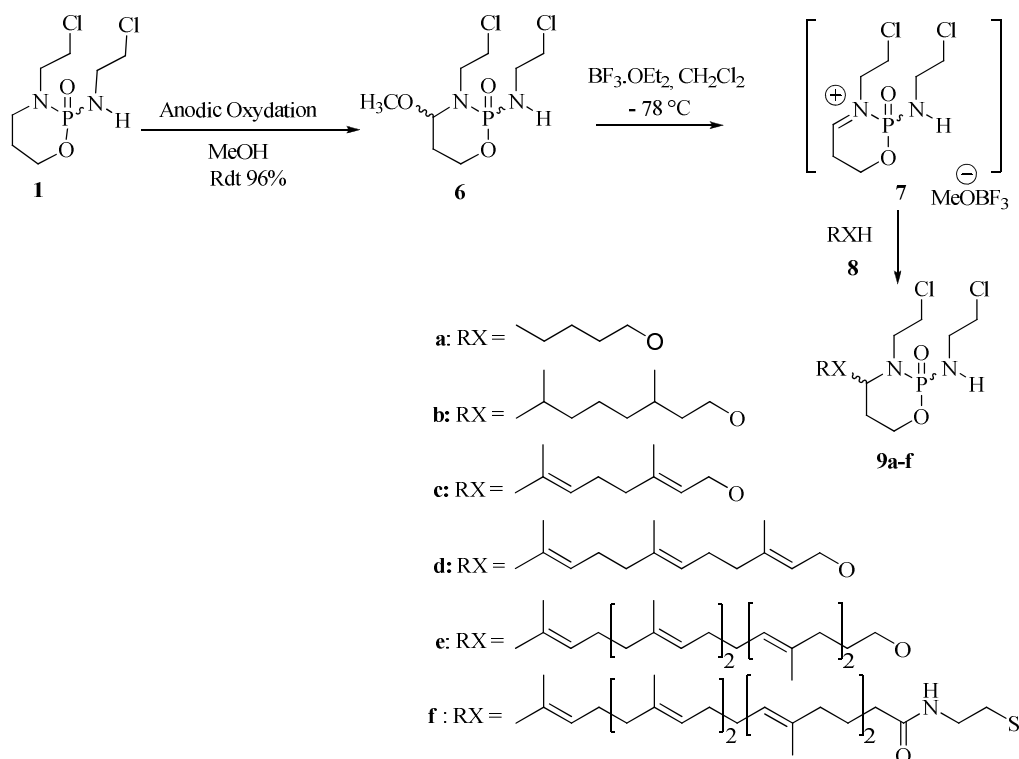
1
2
3 tetrahydrogeranyl group (**9b**) were also synthesized. The nano-assembly formulation of the pre-
4 activated IFO derivatives and the *in vitro* cytotoxic activities on a panel of cancer lines of the
5 NAs are also reported including *in vitro* investigations concerning the release of the key
6 metabolite, i.e. 4-HO-IFO in mice plasma.
7
8
9
10
11

12 13 14 15 **2. Results**

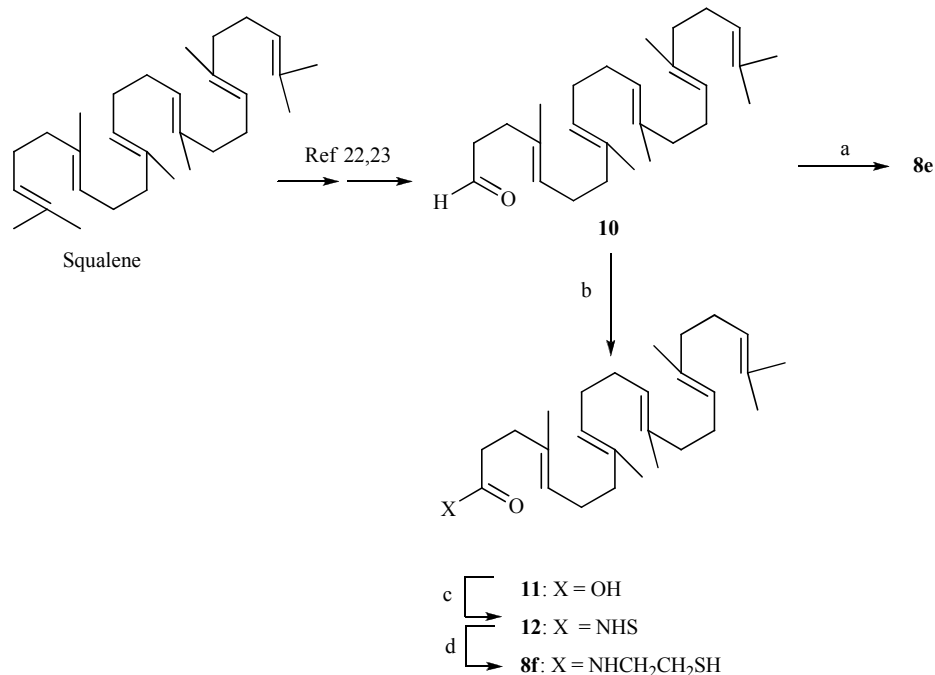
16 17 18 2.1. Chemistry.

19
20 The synthesis of pre-activated conjugates **9a-f** is depicted in **Scheme 2**. According to our
21 previous finding, anodic oxidation of IFO in methanol afforded the expected
22 4-methoxy-ifosfamide (MeO-IFO, **6**) as a mixture of isomers with an optimized yield of 96%.¹¹
23
24 The substitution of the methoxy group by the relevant alkyl chain took advantage of the
25 formation of the iminium salt **7** upon Lewis acid treatment of **6**. A short screening of the Lewis
26 acids (TMSOTf, Ti(OEt)₄, TiCl₄, BF₃.Et₂O) showed that BF₃.Et₂O was the most efficient reagent.
27
28 Thus, treatment of **6** at -78 °C by one equivalent of BF₃.Et₂O followed by addition of a slight
29 excess of nucleophiles **8a-f** gave compounds **9a-f** in 25-53% yield. All pre-activated IFO
30 derivatives were stable enough to be purified by chromatography on silica gel. However a
31 substantial loss of material was observed with the less lipophilic derivatives **9a-c** that accounted
32 for their reduced yields. Conjugates **9a-f** were characterized by ¹H, ¹³C, ³¹P NMR, MS and
33 HRMS. All compounds were shown to be obtained as diastereomeric mixtures due to the
34 presence of the phosphorous stereogenic center together with the C-4 asymmetric center.
35
36
37
38
39
40
41
42
43
44
45
46
47
48
49
50
51
52
53
54
55
56
57
58
59
60

Scheme 2: Synthesis of the pre-activated conjugates **9a-f**.



Alcohols **8a-d** were commercially available, whereas squalene derivatives **8e,f** were obtained by synthesis from squalene and depicted in **Scheme 3**. The synthesis of 1,1',2-trisnorsqualenol (**8e**) was carried out from squalene via 1,1',2-trisnorsqualenic aldehyde (**10**) according to previously reported methods.^{23,24} On the other hand, oxidation of aldehyde **10** gave the known 1,1',2-trisnorsqualenic acid (**11**).²³ Acid activation by NHS using DCC as coupling agent, followed by simple cysteamine treatment afforded **9f** in 72% overall yield.

Scheme 3: Synthesis of the squalenyl appendages **8e,f**.

^a Reagents and conditions : (a) NaBH₄, EtOH, 20 °C, 0.5 h; (b) CrO₃, H₂SO₄, acetone 0°C; (c) NHS, DCC, THF, 20 °C, 24 h; (d) HSCH₂CH₂NH₂.HCl, Et₃N, CH₂Cl₂, 20 °C, 24h.

2.2. Preparation of supramolecular nano-assemblies.

NAs from prodrugs **9c-f** were prepared at a concentration of 2 mg/mL in a single step by nanoprecipitation, occurring spontaneously by addition of an acetonic solution of the bioconjugate (8 mg/ml) into MilliQ® water under vigorous stirring. Formation of NAs occurred immediately without the use of any surfactant. The organic solvent was then evaporated at room temperature (**9c-f**) under vacuum using a Rotavapor®. Then, NAs colloidal dispersions were stored at 4°C. These NAs that exhibited the characteristic Tyndall effect of colloidal systems had a polydispersity index lower than 0.12 as measured by quasi-elastic light scattering. The mean diameters of the obtained NAs are depicted in Table 1. Interestingly, prodrug **9c** with a short two-isoprene unit appendage gave satisfactory NAs. This finding is in agreement with our

previous results about poly-isoprenoyl conjugates of gemcitabine establishing that two-isoprene units are sufficient to provide conjugates with self-assembling properties.²¹ No significant changes neither in the size nor in the polydispersity index of the NAs **9c-f** were detected over a three day storage period at 4°C. The colloidal stability of **9c-f** could be correlated with the fairly negative Zeta potentials observed ($\xi = -30$ mV for **9c**, $\xi = -20$ mV for **9d**, $\xi = -21$ mV for **9e** and $\xi = -34$ mV for **9f**). Furthermore, these highly hydrolysable compounds were found chemically unchanged by ¹H NMR and by MS after 24 h for **9c** and up to three days for **9d-f**. These results seem to indicate that, within the NAs, the polar head group was protected from the external aqueous medium by the hydrophobic isoprenoid core, and that longer the poly-isoprene chain is more stable the NAs are.

As expected, compounds **9a** and **9b** did not provide any auto-assembling properties, clearly demonstrating that the tri-substituted double bonds of the isoprenoid linker group played a crucial role to provide NAs. NAs of conjugates **9c-f** (2 mg/mL) were characterized using Dynamic Light Scattering (DLS) to determine their size, polydispersity index and zeta potential which are summarized in Table 1.

Table 1: Physico-chemical characteristics of the NAs of prodrugs **9c-f** at 2 mg/mL.

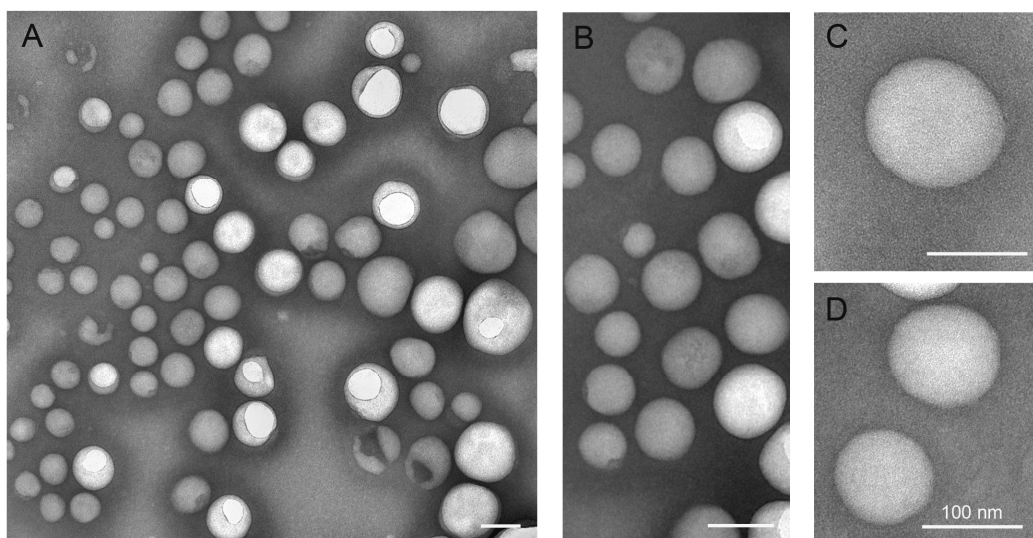
Compound	Mean diameter (nm)	Polydispersity Index (PdI)	Zeta potential (mV)	Drug Loading (%)
9c	126	0.10	-30	63.1
9d	195	0.16	-20	54.2
9e	147	0.12	-21	40.4
9f	167	0.06	-34	36.3

1
2
3 As no surfactant or any excipient was needed to obtain NAs from these materials, the drug
4 loading could be directly deduced from respective molecular mass of the drugs and isoprenoyl
5 moieties. This led to conclude that obtained NAs were characterized by high drug loadings
6 compared to the currently available nano-carriers.
7
8
9
10
11

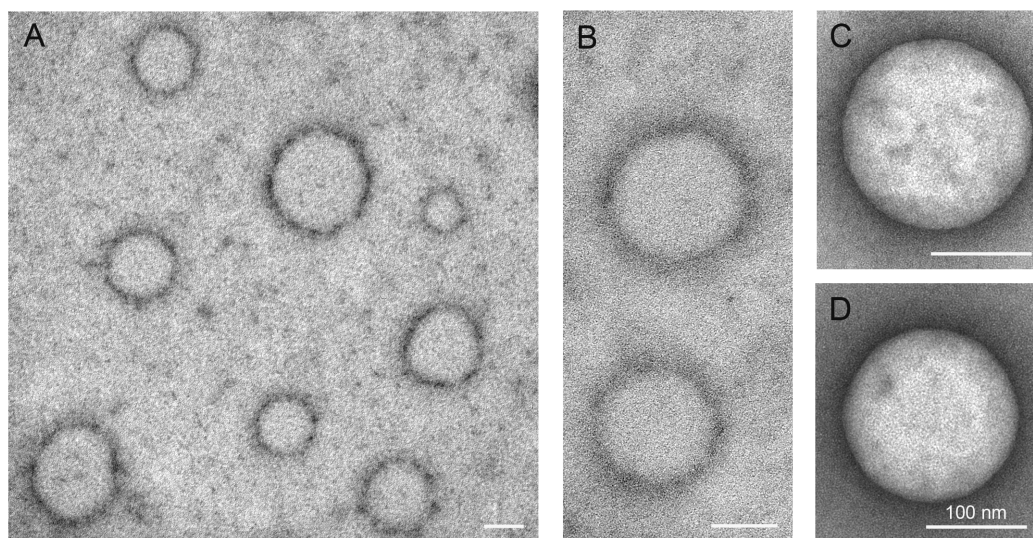
12 2.3. Transmission Electron Microscopy.

13
14
15 Transmission Electron Microscopy (TEM) allowed to characterize individual particles, their
16 shape and their size. However we know that this characterization depends on their spreading
17 onto the grids. We first studied nano-assemblies with conventional negative staining method and
18 we observed spherical shape (150 - 200 nm) as shown in Figure 1), but unusually a few
19 assemblies were present on the grids. We therefore explored others methods by varying the dye
20 or the staining method. Hence, large field of particles could be observed with various sizes (90 –
21 300 nm) which are consistent with measurements by the nanosizer method.
22
23
24
25
26
27
28
29
30
31

32 **Figure 1:** Geranyloxy-IFO NAs suspended in water are observed by transmission electron
33 microscopy using negative staining method by phosphotungstic acid solution. Magnification : A)
34 50,000; B) 85,000; C) and D) 140,000. scale bar : 100 nm.
35
36
37
38
39
40



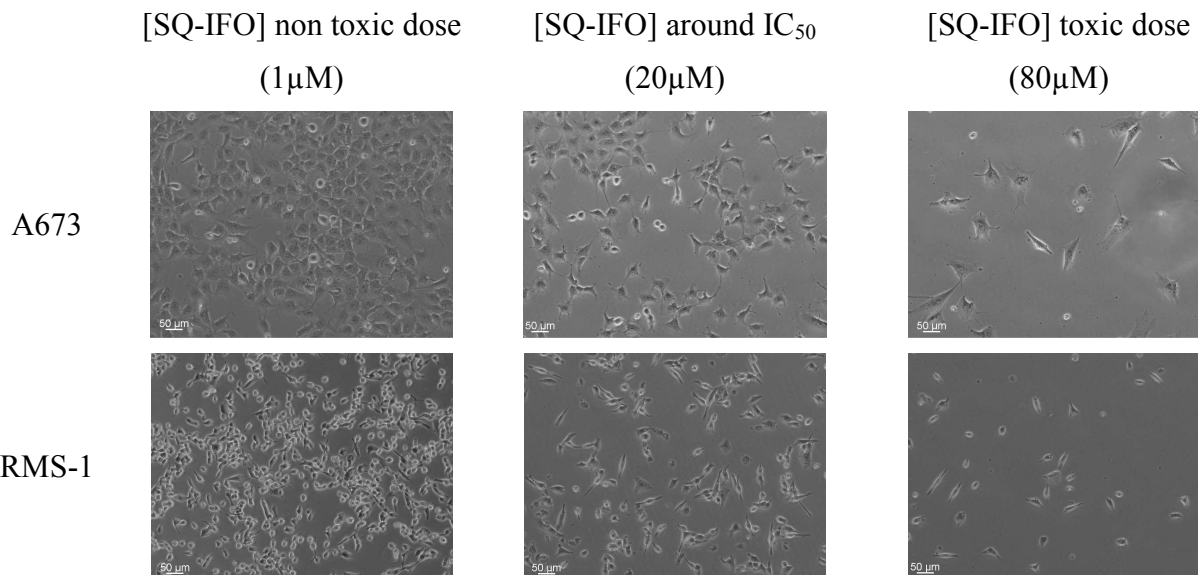
1
2
3 **Figure 2:** Farnesyloxy-IFO NAs suspended in water observed by transmission electron
4 microscopy using positive staining method (A, B) or by negative staining method (C, D).
5
6
7
8 Magnification: A) 50,000; B) 85,000; C) and D) 140,000 - scale bar: 100 nm.
9
10



36 2.4. In vitro cytotoxic evaluation

37 *In vitro* cytotoxicity of compounds **6**, **9a-f** has been tested on Rhabdomyosarcoma (RMS-1) and
38 Ewing sarcoma (A673) cell lines by MTS assay, using IFO as a control. In the absence of
39 cytochrome, IFO showed no activity, whereas all the pre-activated compounds, either as bulk
40 form or as NAs, demonstrated cytotoxic activities (Table 2) with IC_{50} ranging from 0.6 μ M to
41 31.4 μ M. This inhibition is shown in Figure 2 which depicts the action of different SQ-IFO
42 concentrations on the cell proliferation of both cell lines after a 72h treatment. At a low
43 concentration (1 μ M) there is no inhibition of cell growth, whereas the concentrations of 20 and
44 80 μ M show an inhibition cell of 50 and 80%, respectively.
45
46
47
48
49
50
51
52
53
54

55 **Figure 3:** Illustration of SQ-IFO (**9e**) cytotoxicity on RMS-1 and A673 cell lines after 72h
56 incubation.
57
58
59
60



24 All these pre-activated compounds showed a cytotoxic activity after 72h incubation for the tested
25 cell lines, except **9b**, which needed to be incubated as long as 96h to reach its IC₅₀. Surprisingly,
26 for the two cell lines, the NAs formulation of compound **9c** led to a significant improved activity
27 by comparing the IC₅₀ obtained as bulk form (Table 2).
28
29
30
31
32

33
34
35
36 **Table 2:** Cytotoxic activities of IFO derivatives on Ewing sarcoma (A673) and
37 Rhabdomyosarcoma (RMS-1) cell lines (n=3).
38

39
40
41
42
43
44
45
46
47
48
49
50
51
52
53
54
55
56
57

Compound	In vitro Activity (IC ₅₀ μM)	
	A673	RMS-1
6	1.5 ± 0.5	3.8 ± 1.4
9a	17.7 ± 2.3	5.3 ± 1.7
9b**	24.5 ± 2.1	11.3 ± 5.8
9c	25.3 ± 1.5	9.3 ± 4.2
9c NAs	14.7 ± 5.0	0.6 ± 0.2
9d NAs	18.7 ± 3.6	12.3 ± 2.0
9e NAs	22.0 ± 5.	11.4 ± 5.0
9f NAs	23.2 ± 1.3	31.4 ± 4.7*

58 (*) value obtained with the RD rhabdomyosarcoma cell line; (**) 96 h incubation
59
60

The NAs squalenoyl prodrugs **9e** and **9f** were previously evaluated on a panel of cancer cell lines (Table 3). As usually observed with other squalene conjugates, owing to their prodrug nature, **9e** and **9f** displayed variable activities on most cell lines.

Table 3: Cytotoxic activities of poly-isoprenoyl prodrugs NAs (**9e,f**) on various cancer cell lines (n=4).

Cell line	<i>In vitro</i> Activity (IC ₅₀ μM)	
	9e NAs	9f NAs
RD	37.0 ± 1.0	31.4 ± 4.7
SK-N-MC	31.5 ± 1.1	23.1 ± 1.1
UW-479	65.2 ± 1.1	30.5 ± 1.1
SAOS-2	139.1 ± 0.9	31.1 ± 4.0
MCF-7 MDR	157.0 ± 52.2	119.0 ± 27.1
MCF-7	160.9 ± 78.2	45.6 ± 23.2
A549	158.1 ± 83.8	38.6 ± 22.3
M109	>200	22.0 ± 8.6
KB 3.1	128.5 ± 52.7	35.4 ± 21.6
B16F10	134.5 ± 41.9	23.0 ± 4.3
MiaPaCA-2	132.1 ± 67.9	15.5 ± 8.4

Regarding cytotoxic activities of SQ-IFO (**9e**) and SQ-thio-IFO (**9f**), both compounds were active on rhabdomyosarcoma (RD) and neuroblastoma (SK-N-MC). SQ-IFO (**9e**) activity on the other cell lines was poor as IC₅₀ were above 50.0 μM (Table 3). However, it can be underline that SQ-thio-IFO (**9f**) showed interesting activities on glioma (UW-479), osteosarcoma (SAOS-2), lung cancer (M109) melanoma (B16F10) and pancreatic cancer (MiaPaCa-2) cell lines with similar activities ranging between 15.5 to 23.0 μM (Table 3). Moreover, SQ-thio-IFO (**9f**)

1
2
3 showed intermediate cytotoxic activities on the other cell lines but reverse the multidrug
4 resistance on the breast cell line (MCF-7 MDR) as shown in Table 3.
5
6
7
8
9

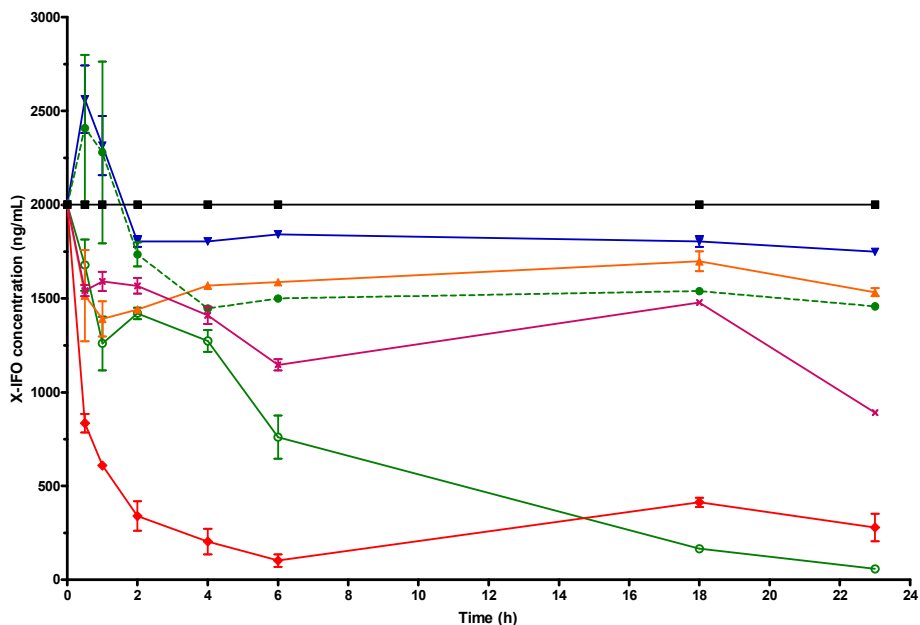
10 11 2.5. In vitro release of 4-HO-IFO from X-IFO prodrugs.

12
13
14 The release kinetic study of the 4-HO-IFO (**2**) from the pre-activated compounds (**6**, **9b-f**) was
15 performed over 24 h in mice plasma incubated at 37°C. All pre-activated IFO compounds (**6**, **9b-**
16 **f**) were studied using stock solutions in ACN. The concentrations of 4-HO-IFO and of the pre-
17 activated compounds were assessed in mice plasma using a quantitative HPLC-MS/MS assay
18 and allowed to display the decrease profile of the pre-activated compounds (**6**, **9b-f**) and the
19 appearance profile of the 4-HO-IFO metabolite concentrations, both expressed in ng/mL, taking
20 into account that the 4-HO-IFO compound was analyzed as the semicarbazone derivative. The
21 kinetics curves show that 4-HO-IFO was indeed produced from all these pre-activated
22 derivatives, except for **9f**. The Figure 4 shows the results obtained with the bulk form of the pre-
23 activated compounds. On one hand, it was observed that concentrations of **9b** (13,17-
24 dimethyloctyloxy-IFO), **9c** (geranyloxy-IFO), **9d** (farnesyloxy-IFO) and **9e** (SQ-IFO) decreased
25 especially during the first two hours and then remained stable, as shown in Figure 4A. On
26 another hand, the concentration of compound **6** (MeO-IFO) decreased quickly during the first
27 two hours and became very low after the 6th hour. Moreover, for compound **9f** (SQ-thio-IFO),
28 the concentration decreased gradually to reach a low value after 23h of incubation. The Figure
29 4B shows the appearance curves of released 4-HO-IFO from each X-IFO compound. We
30 observed that the compound **6** provided increasing 4-HO-IFO concentrations after 2h with a
31 maximum value of 1250 ng/mL, and then slowly decreased until 23h. After 0.5h, compounds **9b**
32 and **9d** produced maximum 4-HO-IFO concentrations of 200 and 700 ng/mL, respectively.
33
34
35
36
37
38
39
40
41
42
43
44
45
46
47
48
49
50
51
52
53
54
55
56
57
58
59
60

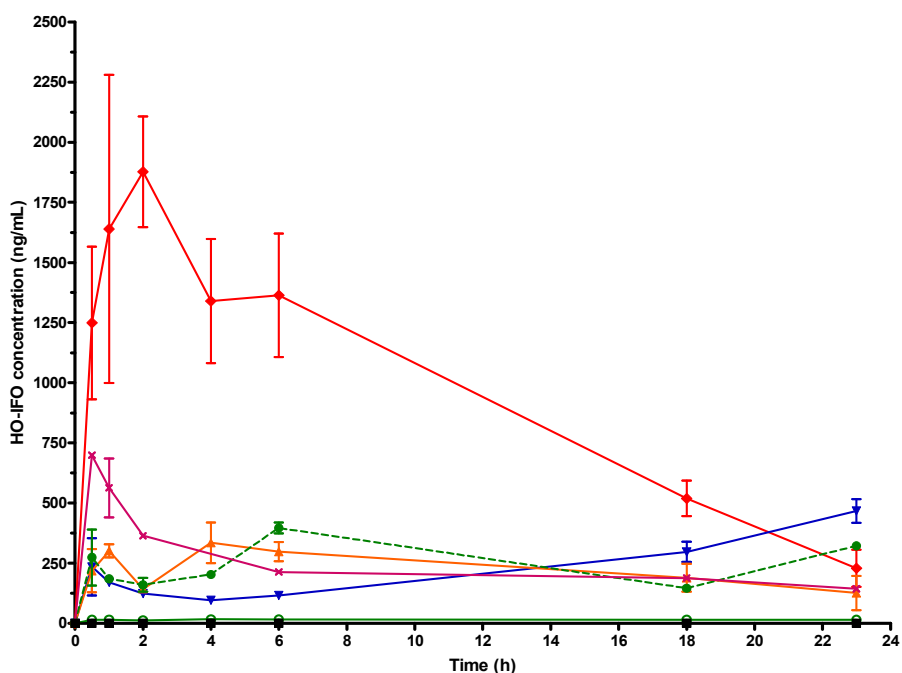
1
2
3 Compounds **9c** and **9e** displayed 4-HO-IFO concentrations of 350 and 400 ng/mL after 4 and 6h,
4
5 respectively. By contrast, concentration lower than 30 ng/mL (at the bottom of Figure 4B) were
6
7 detected with compound **9f** in which the alkoxy group is replaced by an alkylsulfanyl residue.
8
9
10
11
12
13
14
15
16
17
18
19
20
21
22
23
24
25
26
27
28
29
30
31
32
33
34
35
36
37
38
39
40
41
42
43
44
45
46
47
48
49
50
51
52
53
54
55
56
57
58
59
60

Figure 4: Release study of 4-HO-IFO from X-IFO as bulk form in mice plasma incubated at 37°C for 24h. (♦ **6** (MeO-IFO), ▼ **9b** (13, 17-dimethyloctyloxy-IFO), ▲ **9c** (geranyloxy-IFO), × **9d** (farnesyloxy-IFO), ● **9e** (SQ-IFO), ○ **9f** (SQ-thio-IFO and ■ **1** (IFO)): Time-concentration profiles of X-IFO A) and of 4-HO-IFO B).

A)



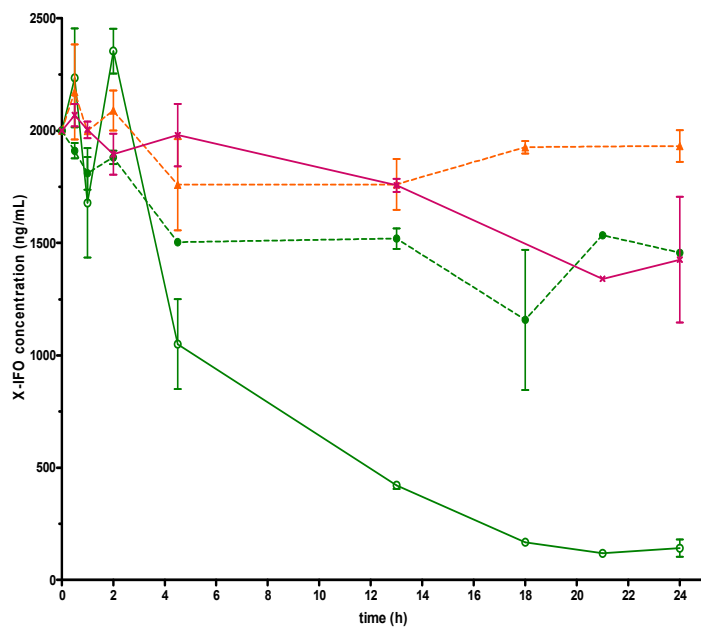
B)



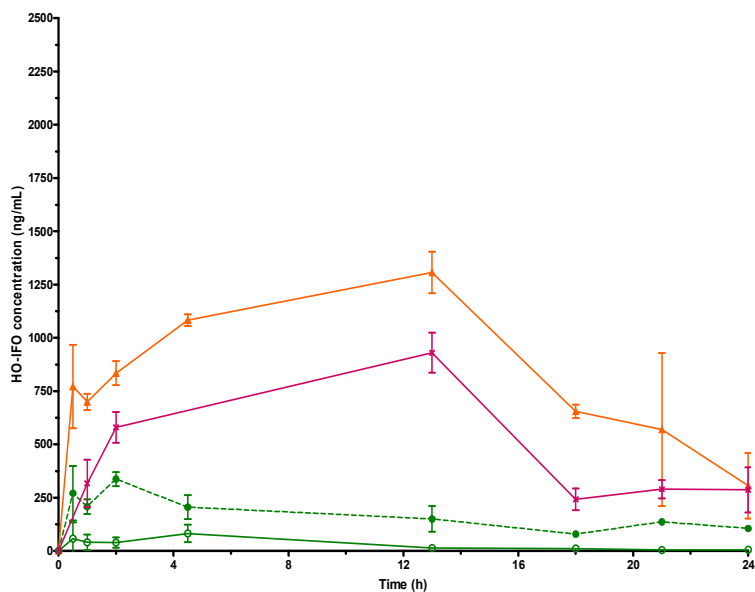
1
2
3 Figure 5A) shows the time-concentration profile obtained for the compounds **9c-f** prepared as
4 NAs. Concentrations of compounds **9c-e** first decreased for 4.5 h and then remained stable for
5
6 24h. Regarding compound **9f**, its concentration decreased gradually and reached a minimum
7
8 value after 24h. Figure 5B) shows the formation of released 4-HO-IFO from the NAs of the pre-
9
10 activated compounds. It was observed that both compounds **9c** and **9d** produced after 13h
11
12 incubation a maximum 4-HO-IFO concentration of 1300 and 900 ng/mL respectively. On the
13
14 other hand, compounds **9e** and **9f** could release low concentrations of 4-HO-IFO with
15
16 concentration of 350 ng/mL after 2h and 100 ng/mL after 4.5h, respectively.
17
18
19
20
21
22
23
24
25
26
27
28
29
30
31
32
33
34
35
36
37
38
39
40
41
42
43
44
45
46
47
48
49
50
51
52
53
54
55
56
57
58
59
60

Figure 5: Release study of 4-HO-IFO from X-IFO as NAs in mice plasma incubated at 37°C for 24h. (▲ 9c (geranyloxy-IFO), × 9d (farnesyloxy-IFI), ● 9e (SQ-IFO) and ○ 9f (SQ-thio-IFO): Time-concentration profiles of X-IFO A) and of 4-HO-IFO B).

A)



B)



3. Discussion and Conclusion.

The pharmacomodulation strategy described herein of IFO has led to the synthesis of seven new pre-activated IFO derivatives (MeO-IFO **6**, pentyloxy-IFO **9a**, 13,17-dimethyloctyloxy-IFO **9b**, geranyloxy-IFO **9c**, farnesyloxy-IFO **9d**, SQ-IFO **9e** and SQ-thio-IFO **9f**). The engraftment of geraniol, farnesol, squalenol or squalenecysteamide to IFO allowed obtaining four compounds, which were able to self-assemble into NAs.

As described previously,¹¹ the *in vitro* cytotoxicity of MeO-IFO (**6**) in absence of cytochrome was similar to IFO with CYP bio-activation. Concerning the other pre-activated IFO derivatives, the *in vitro* cytotoxic studies demonstrated their activity in the same range, with IC₅₀ between 0.6 and 31.4 μM, as expected. Indeed, the aim of this strategy was not to improve their intrinsic cytotoxic activity as the released entity (4-HO-IFO) is the same for all these pre-activated compounds. The aim was to control the delivery of the active agent through the modulation of its release depending on the properties of the engrafted moieties.

It was shown that 72h-incubation were needed for the determination of the IC₅₀, except for 13,17-dimethyloctyloxy-IFO (**9b**), which seemed to act more slowly, as IC₅₀ was reached after 96h. This may be tentatively explained by the increased steric hindrance due to the branched methyl group in the 3' position of the alkyl appendage. Such configuration could significantly modify the release kinetics of the key entity (4-HO-IFO). Concerning the *in vitro* kinetic study of 4-HO-IFO release, we demonstrated that all the pre-activated IFO derivatives produced the key entity leading to the isophosphoramidate mustard, as they were designed for this purpose. Nevertheless, SQ-thio-IFO (**9f**) was not hydrolyzed into 4-HO-IFO, likely due to the different type of bound linkage between the squalenecysteamide and IFO: a sulfide rather than an ether bound is present in the case of the other compounds (**6**, **9a-e**). The relative hydrolytic stability of

1
2
3 **9f** in respect to the *O*-alkyl derivatives **9a-e** could be attributed to the unfavorable protonation of
4 the soft sulfur center, *S*-ethers being weaker bases than *O*-ether.
5
6

7
8 All studied prodrugs were obtained as diastomeric mixtures as evidenced by ³¹P and ¹³C NMR.
9
10 Although each isomer could potentially release the parent drug at different rates, we chose to
11 evaluate the mixture as racemic without separation for two reasons: one of the reasons was that
12 these acid-sensitive prodrugs do not crystallize and must be separated by chromatography
13 leading to a substantial loss of material. However, the main reason was that the mechanism
14 leading to the formation of the 4-OH-IFO metabolite does not involve any enzymatic process but
15 is a simple acid catalyzed hemiaminal ether hydrolysis via protonation, leading to the release of
16 the 4-*O*-alkyl side-chain moiety with formation of an iminium ion and water addition. Thus, the
17 C-4 asymmetric center disappears in this process and the subsequent water addition on the
18 iminium ion would be expected to give 4-OH-IFO. Moreover, the produg stereochemistry
19 corresponds to the one observed in the metabolites resulting of CYP3A4 mediated bioactivation
20 of IFO (see Scheme 1) because 4-OH-IFO is in equilibrium with the ring-opened aldo-
21 isophosphoramidate which leads to epimerization of the C-4 center in the more stable
22 stereochemistry. The hypothesis that the C-4 stereogenic center of these prodrugs displays only a
23 small influence on the cytotoxicity has been reinforced by the observation that both 4-MeO-IFO
24 isomers were found to have very similar cytotoxicity on carcinoma KB cell line (20 and 22 μM
25 respectively).¹¹ This result could probably be related to the axial conformation of the methoxy
26 group in both diastereomers differing only by the conformation of the phosphoryl (P=O) bond.
27 Similarly, we can postulate that the *O*-alkyl groups engrafted in the C-4 position of these
28 prodrugs are in the same axial position due to stereoelectronic control in the addition step. Thus,
29 the same unique relationship with the nitrogen lone pair in both isomers should lead to roughly
30
31
32
33
34
35
36
37
38
39
40
41
42
43
44
45
46
47
48
49
50
51
52
53
54
55
56
57
58
59
60

1
2
3 similar rate of iminium formation when hydrolyzed. Finally, we have chosen to examine these
4
5 prodrugs in their racemic form since IFO used in the clinic is racemic and because it was
6
7 demonstrated that there is no difference in efficacy through the release of 4-HO-IFO between
8
9 racemic IFO and its enantiomers.²⁵ In addition, when *in vivo* pharmacokinetic (PK) studies were
10
11 performed, no statistically differences of therapeutic concentrations and PK parameters were
12
13 shown between them.²⁶
14
15
16
17
18
19

20
21 Taking into account the results of both studies, all the designed pre-activated compounds were
22
23 active without any CYP bio-activation, contrary to IFO. This observation confirms the proof of
24
25 concept concerning the design of these new pre-activated isoprenic IFO derivatives, as these
26
27 compounds generated directly the key entity leading to the release of the isophosphoramidate
28
29 mustard, as it was previously described by Hohorst¹² and Takamizawa¹³ in the mid 70s. This will
30
31 allow further investigations on the administered dose reduction in order to limit the toxic side
32
33 effects occurring in high dose protocols. Moreover, the NAs formulation of the drug could lead
34
35 to nanomedecines designed for a controlled release of the key entity.¹⁵
36
37
38

39
40 Among the designed compounds, four seemed to stand out by their interesting results. As our
41
42 main goal was to administer a safer drug, the high activity and fast 4-HO-IFO release profile of
43
44 MeO-IFO (**6**) were an impediment for controlling optimal pharmacokinetics development of this
45
46 compound. Due to the lack of stability, the compound MeO-IFO released 4-HO-IFO very
47
48 quickly (Figure 4B), the use of this compound in chemotherapy may be considered as equivalent
49
50 to the direct administration of 4-HO-IFO, implying that **6** may never reach its target and could
51
52 lead to harm the patient. However, compounds **9c-f** have interesting properties as they self-
53
54 assemble into NAs with important drug loading. They also show a gradual 4-HO-IFO release
55
56
57
58
59
60

1
2
3 kinetic profile which could be useful for a future active targeting strategy using nano-assembly
4
5 functionalization.
6
7
8
9

10 The next step of this pharmacomodulation strategy will be first to investigate and to explain the
11 reason of the increased activity of **9c** as NAs, which could be imaged by cell internalization
12 investigations using labelled NAs. Then, the *in vivo* efficacy using human tumor xenografted
13 mice and the toxicological impact of these new pre-activated oxazaphosphorine prodrugs (bulk
14 and NAs) will be further investigated.
15
16
17
18
19
20
21
22
23
24
25
26
27
28
29
30
31
32
33
34
35
36
37
38
39
40
41
42
43
44
45
46
47
48
49
50
51
52
53
54
55
56
57
58
59
60

4. Experimental section.

4.1. Chemistry

4.1.1. General

The structure of the synthesized X-IFO products was characterized by ^1H , ^{13}C and ^{31}P NMR spectra, which were recorded on Bruker Avance 400 (400, 100 and 160MHz, for ^1H , ^{13}C and ^{31}P , respectively) spectrometers (Bruker Daltonik, Bremen, Germany). Recognition of methyl, methylene, methine, and quaternary carbon nuclei in ^{13}C NMR spectra rests on the *J*-modulated spin-echo sequence and DEPT135 experiments. Positive electrospray mass spectra (+ESI-MS) were performed using a QuattroLC[®] mass spectrometer (Waters, Manchester, UK) and high resolution mass spectra (HR-MS) were achieved with ± 3 ppm accuracy with an Agilent 6520 series Q-ToF mass spectrometer (Agilent Technologies, Santa Clara, USA) operating in positive electrospray ionization. The size of the obtained NAs was measured using a Malvern particle size analyzer (Zetasizer[®]). Analytical grade solvents were provided by Carlo Erba (Val-de-Reuil, France). Ifosfamide (Holoxan[®]) was supplied from Baxter (Baxter Healthcare Ltd, Auckland, New Zealand) with 99.5% purity. Borontrifluoride diethyl etherate, squalene, geraniol, pentanol, farnesol trans-trans and 3,7-dimethyloctanol were purchased to Alfa Aesar (Schiltigheim, France). Dichloromethane was distilled over calcium hydride, under nitrogen. All reactions involving air- or water-sensitive compounds were performed under positive nitrogen pressure. Analytical thin-layer chromatography was performed on silica gel 60F₂₅₄ (Merck) and the preparative chromatography was performed using column filled with Silica Gel 60A (Merck, Darmstadt, Germany).

4.1.2. HPLC-MS/MS assay of X-IFO purity

1
2
3 The six synthesized and purified X-IFO products **9a-f** (pentyloxy-IFO, geranyloxy-IFO, 13,17-
4 dimethyloctyloxy-IFO, farnesyloxy-IFO, SQ-IFO, SQ-thio-IFO) could contain the residual
5 product MeO-IFO (**6**) and showed a batch purity of 99%. Purity of each X-IFO batch was
6 calculated using a quantitative HPLC-MS/MS assay of the concentration of MeO-IFO impurity.
7
8 Based on the percentage ratio of MeO-IFO and X-IFO concentrations, purity (%) of X-IFO was
9 expressed as: $P = 100 \times ((1 - c \text{ MeO-IFO} / c \text{ X-IFO}))$.

10
11 Briefly, HPLC-MS/MS analyses of reference MeO-IFO standards (10-400 ng/mL) and X-IFO
12 samples (diluted at 10 $\mu\text{g/mL}$) were performed using a 1100 series HPLC system (Agilent
13 Technologies, Waldbronn, Germany) fitted with an Uptisphere[®] C18 5 μm column, (2.1 \times 100
14 mm). Isocratic elution was achieved with a flow rate of 0.25 mL/min using the mobile phase
15 (acetonitrile/ammonium formate 5mM, 95:5, v/v). The total run time was 16.0 min. Analytes
16 were detected using a QuattroLC[®] triple quadrupole mass spectrometer (Waters, Manchester,
17 UK), operating in the positive electrospray ionization (capillary voltage, 3.5kV and cone voltage,
18 25V) using tandem mass spectrometry with their respective MRM transitions (as example, m/z
19 291 \rightarrow 259 for MeO-IFO (**6**) using argon as collision gas and collision energy of 20 eV. The
20 unknown concentration of MeO-IFO in X-IFO samples was quantified using calibration curve of
21 MeO-IFO standards, thanks to Masslynx[®] software. In the same way, the concentration of the
22 IFO impurity was quantified in the initial MeO-IFO product using HPLC-MS/MS (MRM) using
23 the transition m/z 261 \rightarrow 154 for IFO.
24
25
26
27
28
29
30
31
32
33
34
35
36
37
38
39
40
41
42
43
44
45
46
47
48

49 4.2. Pre-activated drug synthesis

50 4.2.1 Synthesis of MeO-IFO (**6**)

51
52 A solution of ifosfamide (**1**) (200 mg, 0.766 mmol,) and sodium tetrafluoroborate (NaBF₄) (170
53 mg, 1.54 mmol) in methanol (10 mL) was introduced into an undivided cell equipped with two
54
55
56
57
58
59
60

graphite rod electrodes at room temperature. The anodic oxidation was followed by checking the full consumption of the starting material with thin-layer chromatography ($\text{CH}_2\text{Cl}_2/(\text{CH}_3)_2\text{CO}$ (50:50, v/v). After which 3.1 F/mol of electricity was passed into the solution at an intensity of 20 mA, sodium carbonate (100 mg, 1 mmol) was added and the solvent was removed under reduced pressure. The residue was then filtered after dissolution in CH_2Cl_2 . After concentration *in vacuo*, we obtained an oil residue corresponding to 4-methoxy-ifosfamide (4-MeO-IFO) (215 mg, 96% yield). This product was then used as raw material without further purification. ^1H NMR ($(\text{CD}_3)_2\text{CO}$, 400 MHz): δ 1.25 (m, 1 H, $\text{H}_{5\alpha}$), 2.72 (m, 1 H, $\text{H}_{5\beta}$), 3.42 (m, 4 H, H_7 and H_9), 3.52 (m, 4 H, H_{10} and H_8), 3.84 (m, 3 H, $\text{H}_{6\alpha}$ and H_{11}), 4.26 (m, 1 H, $\text{H}_{6\beta}$), 4.62 (td, 1 H, $J=3$ and 21 Hz, H_4). ^{13}C NMR ($(\text{CD}_3)_2\text{CO}$, 100 MHz): δ 29.50 (C_5), 43.29 (C_7), 44.23 (C_8), 45.73 (C_{10}), 49.67 (C_9) 54.79 (C_{11}) 62.36 (C_6), 90.75 (C_4). ^{31}P NMR ($(\text{CD}_3)_2\text{CO}$, 160 MHz): δ 7.73 (s) and 8.40 (s).

MS (+ESI): m/z 291.1 (100%) $[\text{M}+\text{H}]^+$; 293.1 (70%) $[\text{M}+2+\text{H}]^+$.

HRMS (+ESI): m/z 291.0426 ($[\text{M}+\text{H}]^+$ calcd for $\text{C}_8\text{H}_{17}\text{N}_2\text{O}_3\text{P}_1\text{Cl}_2$: 290.0354).

4.2.2. Synthesis of pentyloxy-IFO (**9a**)

To a stirring solution of 4-MeO-IFO (**6**) (200 mg, 0.69 mmol) in anhydrous CH_2Cl_2 (10 mL) was added dropwise $\text{BF}_3\cdot\text{OEt}_2$ (86 μL , 0.69 mmol) under inert atmosphere at -78°C . After 45 minutes, a solution of pentanol (148 μL , 1.37 mmol) in CH_2Cl_2 (0.5 mL) was added dropwise. The mixture was stirred for an additional 1h at -78°C and 10 mL of a saturated Na_2CO_3 solution were added. After extraction with CH_2Cl_2 (3 \times 20 mL), the organic phases were dried over MgSO_4 and concentrated using reduced pressure. The obtained residue was purified by column chromatography (silica gel, $\text{CH}_2\text{Cl}_2/(\text{CH}_3)_2\text{CO}/\text{Et}_3\text{N}$ (95:5:0.5, v/v/v)) to yield **9a** as a yellow oil (90 mg, yield 33%). ^1H NMR ($(\text{CD}_3)_2\text{CO}$, 400 MHz): δ 0.92 (t, 3H, $J = 7.1$ Hz, $\text{O}(\text{CH}_2)_4\text{CH}_3$),

1
2
3 1.30-1.45 (m, 4H, CH₃CH₂CH₂), 1.62 (m, 2H, OCH₂CH₂), 2.02-2.07 (m, 3H, H₅ and NH), 3.16-
4
5 3.30 (m, 2H, OCH₂CH₂), 3.47-3.55 (m, 4H, NCH₂CH₂Cl and NHCH₂CH₂Cl), 3.60-3.65 (m, 2H,
6
7 NCH₂CH₂Cl), 3.70-3.75 (m, 2H, NHCH₂CH₂Cl), 4.05-4.20 (m, 1H, H₆), 4.35-4.50 (m, 1H, H₆),
8
9 4.70-4.80 (dd, 1H, *J* = 20.5 Hz and = 2.9 Hz, H₄). ¹³C NMR ((CD₃)₂CO, 100 MHz): δ 14.3 (CH₃,
10
11 O(CH₂)₄CH₃), 23.2 (CH₂, O(CH₂)₃CH₂CH₃), 29.3 (CH₂, O(CH₂)₂CH₂CH₂CH₃), 30.4 (CH₂,
12
13 OCH₂CH₂(CH₂)₂CH₃), 30.9 (CH₂, C₅), 43.6 (CH₂, NCH₂CH₂Cl), 44.0 (CH₂, NHCH₂CH₂Cl),
14
15 46.6 (CH₂, NHCH₂CH₂Cl), 50.2 (CH₂, NCH₂CH₂Cl), 63.2 (CH₂, C₆), 68.6 (CH₂,
16
17 OCH₂(CH₂)₃CH₃), 89.8 (CH, C₄). ³¹P NMR ((CD₃)₂CO, 160 MHz): δ 7.60 (s) and 8.46 (s).

18
19
20 MS (+ESI): *m/z* 347.1 (100%) [M+H]⁺; 349.1 (70%) [M+2+H]⁺.

21
22 HRMS (+ESI): *m/z* 347.1068 ([M+H]⁺ calcd for C₁₂H₂₅N₂O₃P₁Cl₂: 347.1058).

23 24 25 26 27 4.2.3. Synthesis of 13,17-dimethyloctyloxy-IFO (**9b**)

28
29 To a stirring solution of 4-MeO-IFO (**6**) (200 mg, 0.69 mmol) in anhydrous CH₂Cl₂ (10 mL) was
30
31 added dropwise BF₃.OEt₂ (86 μL, 0.69 mmol) under inert atmosphere at -78°C. After 45
32
33 minutes, 3, 7-dimethyloctanol (262 μL, 1.37 mmol) dissolved in a small volume of CH₂Cl₂ (0.5
34
35 mL) was added dropwise, the mixture was continuously stirred for an additional 1 h. The
36
37 reaction was then stopped by addition at low temperature of 10 mL of a saturated Na₂CO₃
38
39 solution. After extraction with CH₂Cl₂, the organic phases were dried over MgSO₄ and
40
41 concentrated under reduced pressure. The obtained residue was subject to column
42
43 chromatography purification (silica gel, CH₂Cl₂/(CH₃)₂CO/Et₃N (95:5:0.5, v/v/v). The different
44
45 fractions containing the compound of interest were pooled and concentrated under reduced
46
47 pressure to yield a yellow to brown oily residue corresponding to the compound of interest **9c**
48
49 (90 mg, yield 28%). ¹H NMR ((CD₃)₂CO, 400 MHz): δ 0.74 (m, 9H,
50
51 O(CH₂)₂CH(CH₃)(CH₂)₂CH(CH₃)₂), 1.05-1.20 (m, 4H, (CH₂)₂CH(CH₃)₂), 1.60-1.70 (m,
52
53
54
55
56
57
58
59
60

2H,NCH₂CH₂Cl), 2.01-2.07 (m, 2H, H₆), 2.91 (s, 1H, NH), 3.15-3.30 (m, 4H, NCH₂CH₂Cl and NHCH₂CH₂Cl), 3.45-3.60 (m, 4H, NCH₂CH₂Cl and NHCH₂CH₂Cl), 3.64 (m, 2H, H₁₁), 4.05-4.19 (m, 1H, H₅), 4.35-4.50 (m, 1H, H₅), 4.70 (m, 1H, H₄). ¹³C NMR ((CD₃)₂CO, 100 MHz): δ 20.0 (CH₃, CH(CH₃)₂), 23.0 (CH₃, CH(CH₃)₂), 25.4 (CH₃, CH₂CH(CH₃)), 28.7 (CH₃, CH₂(CH₂)₂CH(CH₃)₂), 30.5 (CH₂, C₅), 40.0 (CH₂, NHCH₂CH₂Cl), 43.6 (CH₂, CH₂CH₂CH(CH₃)₂), 44.0 (CH₂, NCH₂CH₂Cl), 46.7 (CH₂, NCH₂CH₂Cl), 49.7 (CH₂, OCH₂CH₂CH(CH₃)), 50.3 (CH₂, NHCH₂CH₂Cl), 63.2 (CH₂, C₆), 66.7 (CH₂, OCH₂CH₂CH(CH₃)), 89.8 (CH, C₄). ³¹P NMR ((CD₃)₂CO, 160 MHz): δ 8.47 (s) and 7.55 (s).

MS (+ESI): *m/z* 417.2 (100%) [M+H]⁺; 419.2 (70%) [M+2+H]⁺.

HRMS (+ESI): *m/z* 417.1828 ([M+H]⁺ Calcd for C₁₇H₃₅N₂O₃P₁Cl₂: 417.1840)

4.2.4. Synthesis of geranyloxy-IFO (**9c**)

To a stirring solution of 4-MeO-IFO (**6**) (200 mg, 0.68 mmol) in anhydrous CH₂Cl₂ (10 mL) was added dropwise BF₃.OEt₂ (86 μL, 0.68 mmol) at -78°C. After 45 minutes, a solution of geraniol (237 μL, 1.37 mmol) in CH₂Cl₂ (0.5 mL) was added dropwise, the mixture was stirred for an additional 1 h at -78 °C and quenched by addition of 10 mL of a saturated Na₂CO₃ solution. After extraction with CH₂Cl₂ (3×20 mL), the combined organic phases were dried over MgSO₄ and concentrated under reduced pressure. The obtained residue was purified by column chromatography (silica gel, CH₂Cl₂/(CH₃)₂CO/Et₃N (95:5:0.5, v/v/v)) to yield **9c** as a yellow oil (80 mg, yield 25%). ¹H NMR ((CD₃)₂CO, 400 MHz): δ 1.62 (s, 3H, HC=C(CH₃)), 1.68 (s, 3H, HC=C(CH₃)₂), 1.72 (s, 3H, HC=C(CH₃)₂), 2.01-2.09 (m, 6H, (CH₂)₂CH=C(CH₃)₂ and CH₂CH=(CH₃)), 2.09-2.16 (m, 2H, H₅), 2.85 (m, 1H, NH), 3.15-3.28 (m, 4H, NCH₂CH₂Cl and NHCH₂CH₂Cl), 3.62-3.67 (m, 2H, NCH₂CH₂Cl), 3.70-3.75 (m, 2H, NHCH₂CH₂Cl), 4.08-4.12 (m, 2H, OCH₂CH=CH(CH₃)), 4.12-4.19 (m, 1H, H₆), 4.39-4.49 (m, 1H, H₆), 4.75 (dt, 1H, *J* =

20.9 Hz and $J = 3.2$ Hz, H₄), 5.12 (tt, 1H, $J = 1.2$ Hz and $J = 6.8$ Hz, CH=C(CH₃)₂), 5.39 (td, 1H, $J = 1.2$ Hz and $J = 6.6$ Hz, OCH₂CH=C(CH₃)). ¹³C NMR ((CD₃)₂CO, 100 MHz): δ 16.7 (CH₃, OCH₂CH=C(CH₃)), 17.8 (CH₃, HC=C(CH₃)₂), 25.9 (CH₃, HC=C(CH₃)₂), 27.2 (CH₂, CH₂CH₂HC=C(CH₃)₂), 31.1 (CH₂, C₅), 40.2 (CH₂, NHCH₂CH₂Cl), 43.6 (CH₂, CH₂CH₂HC=C(CH₃)₂), 44.1 (CH₂, NCH₂CH₂Cl), 46.5 (CH₂, NCH₂CH₂Cl), 50.2 (CH₂, NHCH₂CH₂Cl), 63.3 (CH₂, C₆), 64.9 (CH₂, OCH₂), 88.8 (CH, C₄), 121.7 (CH, OCH₂CH=C(CH₃)), 124.8 ((CH, CH=C(CH₃)₂), 132.1 (C, CH=C(CH₃)₂), 140.9 (C, OCH₂CH=C(CH₃)). ³¹P NMR ((CD₃)₂CO, 160 MHz): δ 8.49 (s) ppm.

MS (+ESI): m/z 413.2 (100%) [M+H]⁺; 415.2 (65%) [M+2+H]⁺.

HRMS (+ESI): m/z 413.1522 ([M+H]⁺ Calcd for C₁₇H₃₁N₂O₃P₁Cl₂: 413.1527).

4.2.5. Synthesis of farnesyloxy-IFO (**9d**)

To a stirring solution of 4-MeO-IFO (**6**) (200 mg, 0.68 mmol) in anhydrous CH₂Cl₂ (10 mL) was added dropwise BF₃.OEt₂ (86 μL, 0.68 mmol) at -78°C. After 45 minutes, a solution of farnesol (343 μL, 1.37 mmol) in CH₂Cl₂ (0.5 mL) was added dropwise, the mixture was stirred for an additional 1h at -78 °C and quenched by addition of 10 mL of a saturated Na₂CO₃ solution. After extraction with CH₂Cl₂ (3×20 mL), the combined organic phases were dried over MgSO₄ and concentrated under reduced pressure. The obtained residue was purified by column chromatography (silica gel, CH₂Cl₂/(CH₃)₂CO/Et₃N (95:5:0.5, v/v/v)) to yield **9d** as a yellow oil (110 mg, yield 33%). ¹H NMR ((CD₃)₂CO, 400 MHz): δ 1.60 (s, 3H, HC=C(CH₃)), 1.62 (s, 3H, HC=C(CH₃)₂), 1.66 (s, 3H, HC=C(CH₃)), 1.71 (s, 3H, HC=C(CH₃)₂), 1.96-2.19 (m, 10H, (CH₂)₂CH=C(CH₃) (CH₂)₂CH=C(CH₃)₂ and H₅), 3.15-3.28 (m, 4H, NCH₂CH₂Cl and NHCH₂CH₂Cl), 3.61-3.68 (m, 2H, NCH₂CH₂Cl), 3.70-3.77 (m, 2H, NHCH₂CH₂Cl), 4.02-4.29 (m, 3H, OCH₂CH=CH(CH₃)) and H₆), 4.39-4.49 (m, 1H, H₆), 4.72-4.81 (dt, 1H, $J = 20.9$ Hz and

1
2
3 $J = 3.2$ Hz, H₄), 5.12 (m, 2H, CH=C(CH₃)CH₂CH₂CH=C(CH₃)₂), 5.37-5.43 (td, 1H, $J = 1.2$ Hz
4 and $J = 6.6$ Hz, OCH₂CH=C(CH₃)). ¹³C NMR ((CD₃)₂CO, 100 MHz): δ 16.8 (CH₃, HC=C(CH₃)),
5 17.9 (CH₃, HC=C(CH₃)), 23.7 (CH₃, HC=C(CH₃)₂), 26.0 (CH₃, HC=C(CH₃)₂), 27.6 (CH₂,
6 CH₂CH₂HC=C(CH₃)₂), 30.7 (CH₂, NHCH₂CH₂Cl), 31.2 (CH₂, C₅), 32.7 (CH₂,
7 CH₂CH₂HC=C(CH₃)), 40.3 (CH₂, CH₂CH₂HC=C(CH₃)), 40.6 (CH₂, NHCH₂CH₂Cl), 43.7 (CH₂,
8 CH₂CH₂HC=C(CH₃)₂), 44.2 (CH₂, NCH₂CH₂Cl), 46.6 (CH₂, NCH₂CH₂Cl), 50.2 (CH₂,
9 NHCH₂CH₂Cl), 63.3 (CH₂, C₆), 65.0 (CH₂, OCH₂), 88.9 (CH, C₄), 121.8 (CH,
10 OCH₂CH=C(CH₃)), 124.9 (CH, CH=C(CH₃)), 125.2 ((CH, CH=C(CH₃)), 131.8 (C,
11 CH=C(CH₃)₂), 136.0 (C, CH=C(CH₃)), 141.1 (C, OCH₂CH=C(CH₃)). ³¹P NMR ((CD₃)₂CO, 160
12 MHz): δ 8.52 (s) and 7.77 (s).

13 MS (+ESI): m/z 481.3 (100%) [M+H]⁺; 483.3 (75%) [M+2+H]⁺.

14 HRMS (+ESI): m/z 481.2143 ([M+H]⁺ Calcd for C₂₂H₃₉N₂O₃P1Cl₂:481.2150).

15 4.2.6. Synthesis of trisnorsqualenol (**8e**)

16 To a stirring solution of 1,1',2-trisnor-squalenic aldehyde (**10**) (1,5 g; 3,9 mmol) in ethanol (9
17 mL) was added portionwise NaBH₄ (145 mg; 3,8 mmol), the mixture was continuously stirred
18 for 30 minutes at room temperature. The reaction was then stopped by addition dropwise of a
19 solution of HCl 2N until pH=3. The solution was concentrated under vaccu and the residue was
20 diluted in water (15 mL). After extraction with AcOEt, the organic phases were dried over
21 MgSO₄ and concentrated under reduced pressure. The obtained residue was purified by column
22 chromatography (silica gel, Petroleum spirit/Et₂O (90:10, v/v). yield a colorless oil of **8d** (1,32 g;
23 88 %). ¹H NMR ((CD₃)₂CO, 400 MHz): δ 1.60 (s, 15H, CH=C(CH₃)), 1.68 (s, 3H,
24 (CH₃)₂C=CH), 2.11-1.95 (m, 20H, CHCH₂CH₂C(CH₃)=CH), 3.61 (t, 2H, $J = 7$ Hz, CH₂CH₂OH),
25 5.20-5.06 (m, 5H, C(CH₃)=CHCH₂). ¹³C NMR ((CD₃)₂CO, 100 MHz): δ 16.0 (2CH₃,
26
27
28
29
30
31
32
33
34
35
36
37
38
39
40
41
42
43
44
45
46
47
48
49
50
51
52
53
54
55
56
57
58
59
60

1
2
3 CH=C(CH₃), 16.2 (2CH₃, CH=C(CH₃)), 17.8 (CH₃, CH=C(CH₃)), 25.8 (CH₃, CH=C(CH₃)₂),
4
5
6 26.7 (CH₂, CHCH₂CH₂C(CH₃)), 26.8 (CH₂, CH₂CH₂C(CH₃)), 26.9 (CH₂, CH₂CH₂C(CH₃)), 28.4
7
8 (2CH₂, CH₂CH₂C(CH₃)), 30.9 (CH₂, CH₂CH₂C(CH₃)), 36.2 (CH₂, CH₂CH₂C(CH₃)), 39.8 (CH₂,
9
10 CH₂CH₂C(CH₃)), 39.9 (2CH₂, CH₂CH₂C(CH₃)), 63.0 (CH₂, CH₂CH₂OH), 124.4 (3CH₂,
11
12 CH₂CH=C(CH₃)), 124.6 (CH₂, CH₂CH=C(CH₃)), 125.0 (CH₂, CH₂CH=C(CH₃)), 131.4 (C,
13
14 CH₂CH=C(CH₃)₂), 134.7 (C, CH₂C(CH₃)=CH), 135.0 (C, CH₂C(CH₃)=CH), 135.1 (C,
15
16 CH₂C(CH₃)=CH), 135.3 (C, CH₂C(CH₃)=CH).
17
18
19

20 4.2.7. Synthesis of SQ-IFO (**9e**)

21
22 To a stirring solution of 4-MeO-IFO (**6**) (200 mg, 0.68 mmol) in distilled CH₂Cl₂ (0.5 mL) was
23
24 added dropwise BF₃.OEt₂ (86 μL, 0.68 mmol) under inert atmosphere at -78 °C. After 10
25
26 minutes, trisnorsqualenol (**8d**) (200 mg, 1.37 mmol) dissolved in a small volume of CH₂Cl₂ (0.5
27
28 mL) was added dropwise, the mixture was continuously stirred for an additional 1h. The reaction
29
30 was then stopped by addition at low temperature of 5 mL of a saturated Na₂CO₃ solution. After
31
32 extraction with CH₂Cl₂ the organic phase was dried over MgSO₄ and concentrated under reduced
33
34 pressure. The obtained residue was subject to column chromatography purification (silica gel,
35
36 CH₂Cl₂/MeOH/Et₃N (98:2:0.1, v/v/v)). To yield **9d** as a yellow oil (120 mg, yield 27%). ¹H
37
38 NMR ((CD₃)₂CO, 400 MHz): δ 1.61 (s, 3H, CH=C(CH₃)), 1.64 (s, 12H, CH=C(CH₃)), 1.68 (s,
39
40 3H, (CH₃)₂C=CH), 1.78-1.72 (m, 2H, CH₂CH₂CH₂O), 2.19-1.97 (m, 20H, 9CH₂ and H₅), 3.33-
41
42 3.16 (m, 3H, NHCH₂CH₂Cl and H₇), 3.58-3.43 (m, 3H, H₇, CH₂CH₂CH₂O), 3.66 (t, J = 6 Hz,
43
44 2H, NHCH₂CH₂Cl), 3.80-3.71 (m, 2H, NCH₂CH₂Cl), 4.00-3.90 (m, 1H, NH), 4.21-4.09 (m, 1H,
45
46 H₆), 4.50-4.38 (m, 1H, H₆), 4.75 and 4.70 (2 t, J = 4 Hz, 1H, H₄), 5.24-5.09 (m, 5H,
47
48 (CH₃)C=CHCH₂). ¹³C NMR ((CD₃)₂CO, 100 MHz): δ 16.1 (2CH₃, CH₂CH=C(CH₃)), 16.2
49
50 (2CH₃, CH₂CH=C(CH₃)), 17.8 (CH₃, CH₂CH=C(CH₃)), 25.9 (CH₃, (CH₃)₂C=CH), 27.3 (CH₂),
51
52
53
54
55
56
57
58
59
60

1
2
3 27.4 (CH₂), 27.5 (CH₂), 28.9 (3CH₂), 32.2 (CH₂), 36.7 (CH₂), 40.5 (3CH₂), 43.5 (CH₂,
4 NHCH₂CH₂Cl), 44.0 (CH₂, NCH₂CH₂Cl), 46.6 (CH₂, NHCH₂CH₂Cl), 50.2 (CH₂, NCH₂CH₂Cl),
5
6
7 63.2 (CH₂, C₆), 68.1 (CH₂), 89.7 (CH, C₄), 124.9 (CH, (CH₃)C=CHCH₂), 125.0 (CH,
8 (CH₃)C=CHCH₂), 125.1 (CH, (CH₃)C=CHCH₂), 125.2 (2CH, (CH₃)C=CHCH₂), 131.6 (C,
9 (CH₃)C=CHCH₂), 135.0 (C, (CH₃)C=CHCH₂), 135.4 (C, (CH₃)C=CHCH₂), 135.6 (2C,
10 (CH₃)C=CHCH₂). ³¹P NMR ((CD₃)₂CO, 160 MHz): δ 10.65 (s), 10.25 (s).

11
12
13 MS (+ESI): *m/z* 645.3 (100%) [M+H]⁺; 647.3 (72%) [M+2+H]⁺.

14
15
16 HRMS (+ESI): *m/z* 645.3710 ([M+H]⁺ Calcd for C₃₄H₅₉N₂O₃P₁Cl₂: 645.3718).

17 18 19 20 21 22 23 4.2.8. Synthesis of *N*-(mercaptoethyl)-squalenamide (**8f**)

24
25 To a solution of 1,1',2'- trisnorsqualenic acid **11** (910 mg; 2.02 mmol) in THF (16 mL) were
26
27 added NHS (240 mg, 2.08 mmol) and DCC (416 mg; 2.02 mmol). The reaction mixture was
28
29 stirred at room temperature for 24h and filtered. The filtrate was concentrated under reduced
30
31 pressure and the residue was taken up into CH₂Cl₂ (12 mL). Triethylamine (560 mg, 5.80 mmol)
32
33 and cysteamine hydrochloride (660 mg; 5.80 mmol) were then added and the reaction mixture
34
35 was stirred for 24h. Water (5 mL) was added and the mixture was extracted with ethyl acetate
36
37 (3×20 mL). The combined organic layers were washed with 1N HCl (2×10 mL) and brine (10
38
39 mL). The organic phase was dried over MgSO₄ and concentrated under reduced pressure. The
40
41 residue was purified by column chromatography (silica gel, petroleum spirit/AcOEt, (3:1, v/v))
42
43 to give **8e** as a colorless oil (660 mg, 72 %). ¹H NMR ((CD₃)₂CO, 400 MHz): δ 1.60 (s, 12H,
44
45 CH₂CH=C(CH₃)), 1.62 (s, 3H, CH₂CH=C(CH₃)), 1.68 (s, 3H, (CH₃)₂C=CH), 2.11-1.96 (m, 16H,
46
47 CH₂CH₂C(CH₃)=), 2.29 (s, 4H, NH(O=)CCH₂CH₂C(CH₃)=), 2.62 (td, 2H, *J* = 7 Hz and *J* = 2
48
49 Hz, NHCH₂CH₂SH), 3.40 (m, 2H, NHCH₂CH₂SH), 5.20-5.05 (m, 5H, (CH₃)C=CHCH₂), 5.94 (s
50
51 large, 1H, NH). ¹³C NMR ((CD₃)₂CO, 100 MHz): δ 16.1 (2 CH₃, CH₂CH=C(CH₃)), 16.2 (2CH₃,
52
53
54
55
56
57
58
59
60

1
2
3 CH₂CH=C(CH₃)), 17.8 (CH₃, CH₂CH=C(CH₃)), 24.9 (CH₂), 25.9 (CH₃, CH=C(CH₃)₂), 26.8
4 (2CH₂), 26.9 (CH₂), 28.4 (2CH₂), 35.3 (CH₂), 35.4 (CH₂), 39.7 (CH₂), 39.9 (2CH₂), 42.4 (CH₂),
5
6
7
8 124.5 (CH, (CH₃)C=CHCH₂), 124.6 (CH, (CH₃)C=CHCH₂), 125.7 (CH, (CH₃)C=CHCH₂), 125.7
9
10 (CH, (CH₃)C=CHCH₂), 131.4 (C, (CH₃)C=CHCH₂), 133.6 (C, (CH₃)C=CHCH₂), 135.0 (C,
11
12 (CH₃)C=CHCH₂), 135.1 (C, (CH₃)C=CHCH₂), 135.3 (C, (CH₃)C=CHCH₂), 173.0 (C, NHC=O).
13
14

15 4.2.9. Synthesis of SQ-thio-IFO (**9f**)

16
17 To a stirring solution of 4-MeO-IFO (**6**) (200 mg, 0.68 mmol) in distilled CH₂Cl₂ (0.5 mL) was
18 added dropwise BF₃.OEt₂ (86 μL, 0.68 mmol) under inert atmosphere at -78°C. After 10
19 minutes, *N*-(mercaptoethyl)-squalenamamide **8e** (660 mg, 1.37 mmol) dissolved in a small volume
20 of CH₂Cl₂ (0.7 mL) was added dropwise, the mixture was continuously stirred for an additional
21 1h. The reaction was then stopped by addition at low temperature of 5 mL of a saturated Na₂CO₃
22 solution. After extraction with CH₂Cl₂ the organic phase was dried over MgSO₄ and concentrated
23 under reduced pressure. The obtained residue was purified by column chromatography (silica
24 gel, CH₂Cl₂/MeOH/Et₃N (98:2:0.1, v/v/v)). The different fractions containing the compound of
25 interest were pooled and concentrated under reduced pressure to yield a yellow to brown oily
26 residue corresponding to the compound of interest **9e** (98 mg, yield 20%). ¹H NMR ((CD₃)₂CO,
27 400 MHz): δ 1.59 (s, 3H, CH₂CH=C(CH₃)), 1.61 (s, 12H, CH₂CH=C(CH₃)), 1.66 (s, 3H,
28 (CH₃)₂C=CH), 2.14-1.96 (m, 17H, CH₂(CH₃)C=, CH₂CH=C(CH₃), H₅), 2.26 (s, 4H,
29 (CH₃)CCH₂CH₂C(=O)NH), 2.50-2.38 (m, 1H, H₅), 2.70-2.58 (m, 2H, NHCH₂CH₂S), 3.41-3.18
30 (m, 4H, NHCH₂CH₂Cl, NHCH₂CH₂S), 3.53-3.44 (m, 2H, NCH₂CH₂Cl), 3.62 (t, J = 7 Hz, 2H,
31 NHCH₂CH₂Cl), 3.87-3.76 (m, 2H, NCH₂CH₂Cl), 4.34-4.15 (m, 2H, H₆, NH), 4.80-4.66 (m, 2H,
32 H₄, H₆), 5.24-5.07 (m, 5H, (CH₃)C=CHCH₂), 7.32 (s large, 1H, CONH). ¹³C NMR ((CD₃)₂CO,
33 100 MHz): δ 16.1 (2CH₃, CH=C(CH₃)), 16.2 (2CH₃, CH=C(CH₃)), 17.8 (CH₃, CH=C(CH₃)),
34
35
36
37
38
39
40
41
42
43
44
45
46
47
48
49
50
51
52
53
54
55
56
57
58
59
60

1
2
3 25.9 (CH₃, (CH₃)₂C=CH), 27.3 (CH₂), 27.4 (CH₂), 27.5 (CH₂), 28.9 (3CH₂), 32.6 (CH₂), 31.8
4 (CH₂), 33.4 (CH₂, C₅), 36.3 (CH₂), 35.7 (CH₂), 40.5 (3CH₂), 39.9 (CH₂, NHCH₂CH₂S), 44.2
5 (CH₂, NHCH₂CH₂Cl), 42.6 (CH₂, NCH₂CH₂Cl), 45.8 (CH₂, NHCH₂CH₂Cl), 48.6 (CH₂,
6 NCH₂CH₂Cl), 66.3 (CH, C₄), 124.9 (CH, (CH₃)C=CHCH₂), 125.0 (CH, (CH₃)C=CHCH₂), 125.1
7 (CH, (CH₃)C=CHCH₂), 125.2 (2CH, (CH₃)C=CH), 131.6 (C, (CH₃)C=CH), 135.0 (C,
8 (CH₃)C=CH), 135.5 (C, (CH₃)C=CH), 135.6 (2C, (CH₃)C=CH), 172.8 (C, CONH), 63.9 (CH₂,
9 C₆). ³¹P NMR ((CD₃)₂CO, 160 MHz): δ 8.47 (s) and 7.55 (s).

10
11 MS (+ESI): *m/z* 718.3 (100%) [M+H]⁺; 720.3 (80%) [M+2+H]⁺.

12
13 HRMS (+ESI): *m/z* 718.3692 ([M+H]⁺ Calcd for C₃₆H₆₂N₃O₃P₁S₁Cl₂:718.3705).

14 15 16 17 18 19 20 21 22 23 24 25 26 27 4.3. Preparation and characterization of pre-activated drug nano-assemblies.

28 Geranyloxy-IFO (**9c**), farnesyloxy-IFO (**9d**), SQ-IFO (**9e**) and SQ-thio-IFO (**9f**) NAs were
29 prepared by nanoprecipitation as follows. The purified product was dissolved in acetone at a
30 concentration of 8 mg/mL. This solution was then added dropwise into Milli-Q water under
31 magnetic stirring to obtain a final 2 mg/mL concentration. The acetone was then evaporated
32 under reduced pressure using a Rotovapor to obtain an aqueous suspension of the pre-activated
33 drug NAs.
34
35
36
37
38
39
40
41
42

43 The hydrodynamic diameter of these NAs was measured at 20 °C by Dynamic Light scattering
44 using a Nanosizer ZS (Malvern Instrument Ltd, France). An amount of 20 μL of the suspension
45 was diluted in 980 μL of Milli-Q water for the analysis of the NAs properties. The results give
46 the mean hydrodynamic diameter of the dispersed NAs from three independent series of ten
47 measurements. The standard deviation and the polydispersity index were also given, moreover
48 the Zeta (ξ) potential was also determined.
49
50
51
52
53
54
55
56
57
58
59
60

4.4. Transmission Electron Microscopy processing.

3 μl of sample, were deposited on a 300-mesh copper grid covered with a thin carbon film, activated by conventional glow-discharge (adapted for negative staining) or in the presence of pentylamine adapted for positive staining.²⁷ Grids were washed with aqueous uranyl acetate 2% (w/v) or with aqueous phosphotungstic acid 0.3% (w/v), dried and observed in zero loss *bright field* mode, using a Zeiss 902 transmission electron microscope. Images were captured at various magnifications (50,000, 85,000 or 140,000) with a Veleta CCD camera (2k x2k) and analyzed with iTEM software (Olympus Soft Imaging Solution).

4.5. Cell lines and cell culture.

Several cancerous cell lines have been used for the *in vitro* evaluation. These cell lines were chosen based on IFO's therapeutic indications. Thirteen cancer cell lines were selected for the cytotoxicity assay as follows: RD (Rhabdomyosarcoma), A673 (human Ewing sarcoma), SK-N-MC (Ewing sarcoma), UW-479 (Glioma), SAOS-2 (Osteosarcoma), MCF-7 (Breast Cancer), MCF-7 MDR (Breast Cancer), A549 (Lung carcinoma), M109 (Lung Carcinoma), KB3.1 (Lung Cancer), B16F10 (Melanoma), MiaPaCa-2 (Pancreatic Cancer) and RMS-1 (human Rhabdomyosarcoma). The cells were grown in DMEM (Dulbecco's Modified Eagle Medium) or RPMI (Roswell Park Memorial Institute medium) supplemented with 10% of fetal calf serum (FCS) and 100 U/mL penicilline and 100 $\mu\text{g}/\text{mL}$ streptomycin at 37 °C in presence 5% CO_2 and 95% hygrometry.

4.6. Cytotoxicity assay.

Cytotoxicity of the different pre-activated drugs has been investigated using the MTS ((3-(4,5-dimethylthiazol-2-yl)-5-(3-carboxymethoxyphenyl)-2-(4-sulfophenyl)-2H-tetrazolium)) method (Promega). The compounds (**6**, **9a-d**) MeO-, pentyloxy-, 13,17-dimethyloctyloxy- geranyloxy-

1
2
3 and farnesyloxy-IFO have been tested on A673 and RMS-1 cell lines, corresponding to
4
5 respectively human Ewing Sarcoma and Rhabdomyosarcoma cell lines. The pre-activated
6
7 prodrugs MeO-IFO (**6**), pentyloxy-IFO (**9a**) and 13, 17-dimethyloctyloxy-IFO (**9b**) were tested
8
9 under bulk form geranyloxy-IFO (**9c**) was tested under bulk and NAs forms and farnesyloxy-IFO
10
11 (**9d**) only as NAs, as the free form was too lipophilic and insoluble in the media to be tested. The
12
13 compounds SQ-IFO (**9e**) and SQ-thio-IFO (**9f**) were tested on 12 other human cell lines: (RD,
14
15 A673, SK-N-MC, UW-479, SAOS-2, MCF-7, MCF-7 MDR, A549, M109 KB3.1, B16F10 and
16
17 MiaPaCa-2) and their cytotoxic activities were evaluated under NAs form.

18
19
20
21
22 The cells were seeded in 96-well plates at optimal cell density determined previously and
23
24 incubated with 100 μ L of DMEM or RPMI containing 10% of FBS and 100 U/mL penicilline
25
26 and 100 μ g/mL streptomycin at 37 °C in presence 5% CO₂ and 95% hygrometry. After 24h, the
27
28 cells were treated with 100 μ L of the different pre-activated prodrugs at different concentrations
29
30 (i.e. 0.1, 0.5, 1, 5, 10, 50, 100, 200 μ M) for all the cell lines. After 72h, or 96h for the compound
31
32 13,17-dimethyloctyloxy-IFO (**9b**), 20 μ L (1/10) of MTS reagent were added in each well.
33
34 Depending on the cell line, 2 to 5h incubations were needed to obtain the optimum optical
35
36 density which was measured at 490 nm wavelength using a microplate reader (EL808, Biotek
37
38 Instrument). Untreated cells were used as control. Each pre-activated drug concentration was
39
40 tested in six replicates. Results show the percentage of living cells compared to the control, and
41
42 the IC₅₀ of each compound regarding the tested cell line was determined using Prism 4 (Graph
43
44 Pad Software, San Diego).

4.7. *In vitro* release of 4-HO-IFO from X-IFO prodrugs by HPLC-MS/MS.

45
46
47 Stock solutions of 4-HO-IFO were produced as described from hydroperoxy-ifosfamide (4-
48
49 HOO-IFO) (Niomech, Germany)²⁸. During sample incubation at 37°C, the 4-HO-IFO compound
50
51
52
53
54
55
56
57
58
59
60

1
2
3 was stabilized in mice plasma (Euromedex, Strasbourg) samples and prepared according to the
4
5 derivatization method using hydrochloride semi-carbazide reagent (SCZ, Fluka)²⁹. Briefly, 1 mL
6
7 plasma in a 2 mL polypropylene tube and 100 μ L solution (SCZ 2M in pH 7.4 buffer) were
8
9 mixed. A volume of 50 μ L of internal standard (100 ng/mL in acetonitrile) was added to a
10
11 sample aliquot of 55 μ L. Liquid/liquid extraction was then performed with 1 mL of methyl *ter*-
12
13 butyl ether. After vortex-mixing, the supernatant was then transferred in another 1.5 mL conic
14
15 tube and evaporated at 35 °C under vacuum. Finally, the extract was dissolved with 200 μ L of
16
17 HPLC solvent and analysed (20 μ L) by HPLC-MS/MS. The RX-IFO compounds and the 4-HO-
18
19 IFO metabolite were quantified simultaneously in mice plasma, over a concentration range from
20
21 50 to 5000 ng/mL, by HPLC-MS/MS using the QuattroLC tandem mass spectrometer (Waters,
22
23 Manchester, UK) operating with positive electrospray ionization and detected with the following
24
25 MRM transitions: m/z 261.0 \rightarrow m/z 154.0 for IFO, m/z 334.0 \rightarrow 221.0 for semicarbazone
26
27 derivative (4-HO-IFO-SCZ), m/z 180.0 \rightarrow 135.0 for hexamethyl phosphoramidate as internal
28
29 standard; m/z 291.0 \rightarrow 259.0 for methoxy-IFO, m/z 413.0 \rightarrow 259.0 for geranyloxy-IFO, m/z
30
31 417.1 \rightarrow 259.0 for 13,17-dimethyloctyloxy-IFO, m/z 481.0 \rightarrow 259.0 for farnesyloxy-IFO, m/z
32
33 645.5 \rightarrow 259.0 for SQ-IFO and m/z 718.3 \rightarrow 259.0 for SQ-thio-IFO. They were analyzed using
34
35 the isocratic eluent (acetonitrile / ammonium formate 5mM, 95:5, v/v) with a Ultrasphere[®] C18
36
37 5 μ m column (2 mm i.d. x 100 mm length (Interchim, Montluçon, France) running at a flow-rate
38
39 of 0.25 mL/min.
40
41
42
43
44
45
46
47
48
49
50
51
52
53
54
55
56
57
58
59
60

Supporting Information.

HPLC-MS/MS chromatograms and high resolution mass spectra (HRMS) of X-IFO compounds (6, 9a-f).

AUTHOR INFORMATION

Corresponding Author

A. P.: Phone: +33 1 42 11 47 30; fax +33 1 42 11 52 77; email: angelo.paci@gustaveroussy.fr.

Funding Sources

The research leading to these results has received funding from the National Research Agency for NanoSqualOnc project: Program P2N, Grant N° NANO 00301.

A three year PhD scholarship has been granted by the Ministry of Higher Education and Research through Doctoral school 425 (Therapeutic innovation: from the fundamental to the applied, University of Paris Sud). Part of this study was granted by Gustave Roussy Foundation thanks to Gustave Roussy Transfer.

ACKNOWLEDGMENT:

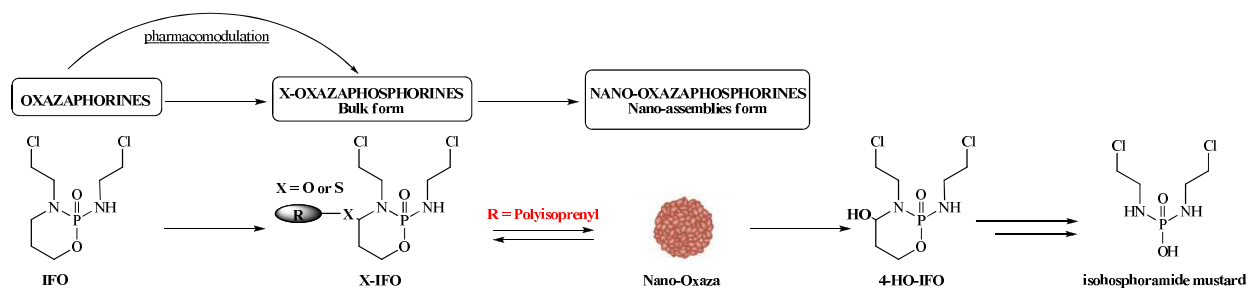
High resolution mass spectra of X-IFO products were performed thanks to Sylvère Durand (Mass Spectrometry metabolomics core facility, Gustave Roussy Cancer Campus Grand Paris).

ABBREVIATIONS

IFO, ifosfamide; Mesna, 2-mercaptoethanesulfonate of sodium; NAs, nano-assemblies; NHS, N-hydroxysuccinimide; Et₃N, triethylamine; ACN, acetonitrile; AcOEt, ethyl acetate; PDI, polydispersity index; RPMI, Roswell Park memorial institute medium; DMEM, Dulbecco's

1
2
3 modified eagle medium; FCS, fetal calf serum; MTS, 3-(4,5-dimethylthiazol-2-yl)-5-(3-
4 carboxymethoxyphenyl)-2-(4-sulfophenyl)-2H-tetrazolium; SCZ, semicarbazide; MRM, multiple
5
6 reaction monitoring; HPLC-MS/MS, high-performance liquid chromatography-tandem mass
7
8 spectrometry.
9
10
11
12
13
14
15
16
17
18
19
20
21
22
23
24
25
26
27
28
29
30
31
32
33
34
35
36
37
38
39
40
41
42
43
44
45
46
47
48
49
50
51
52
53
54
55
56
57
58
59
60

Table of Contents graphic.



REFERENCES

- 1
2
3
4
5
6
7
8
9 (1) Giraud, B.; Hebert, G.; Deroussent, A.; Veal, G. J.; Vassal, G.; Paci, A. Oxazaphosphorines:
10 new therapeutic strategies for an old class of drugs. *Expert Opin. Drug Metab. Toxicol.* **2010**, *6*,
11 919–938.
12
13
14
15
16 (2) Kerbush, T.; Herben, V. M.; Jeuken, M. J.; Ouwkerk, J.; Keizer, H. J.; Beijnen, J. H.
17 Distribution of ifosfamide and metabolites between plasma and erythrocytes. *Biopharm. Drug.*
18 *Dispos.* **2001**, *22*, 99–108.
19
20
21
22
23 (3) Storme, T.; Deroussent, A.; Mercier, L.; Prost, E.; Re, M.; Munier, F.; Martens, T.; Bourget,
24 P.; Vassal, G.; Royer, J.; Paci, A. New ifosfamide analogs designed for lower associated
25 neurotoxicity and nephrotoxicity with modified alkylating kinetics leading to enhanced *in vitro*
26 anticancer activity. *J. Pharmacol. Exp. Ther.* **2009**, *328*, 598–609.
27
28
29
30
31
32 (4) Kobylińska, K.; Koralewski, P.; Sobik, B.; Gasiorek, M.; Kobylińska, M. Pharmacokinetics
33 and toxicity of oral (-)-(S)-bromofosfamide in lung cancer patients. *Arzneimittelforschung.* **2001**,
34 *51*, 600–603.
35
36
37
38
39 (5) Liang, J.; Huang, M.; Yu, X. Q.; Zhou, S. Design of new oxazaphosphorine anticancer drugs.
40 *Curr. Pharm. Des.* **2007**, *13*, 963–978.
41
42
43
44 (6) Zheng, J. J.; Chan, K. K.; Muggia, F.; Preclinical pharmacokinetics and stability of
45 isophosphoramidate mustard. *Cancer Chemother. Pharmacol.* **1994**, *33*, 391–398.
46
47
48
49 (7) Germann, N.; Urien, S.; Rodgers, A. H.; Ratterree, M.; Struck, R. F.; Waud, W. R.;
50 Serota, D. G.; Bastian, G.; Jursic, B. S.; Morgan, L. R. Comparative preclinical toxicology and
51 pharmacology of isophosphoramidate mustard, the active metabolite of ifosfamide. *Cancer*
52 *Chemother. Pharmacol.* **2005**, *55*, 143–151.
53
54
55
56
57
58
59
60

- 1
2
3
4
5 (8) Pohl, J.; Bertram, B.; Hilgard, P.; Nowrousian, M. R.; Stüben, J. A. Sugar-linked
6 isophosphoramidate mustard derivative exploiting transmembrane glucose transport. *Cancer*
7
8 *Chemother. Pharmacol.* **1995**, *35*, 364–370.
9
10
11
12 (9) Lacombe, D. Glufosfamide: can we improve the process of anticancer agent development?
13
14 *Expert Opin. Investig. Drugs.* **2012**, *21*, 749-754.
15
16
17 (10) Blaney, S. M.; Boyett, J.; Friedman, H.; Gajjar, A.; Geyer, R.; Horowitz, M.; Hunt, D.;
18
19 Kieran, M.; Kun, L.; Packer, R.; Phillips, P.; Pollack, I. F.; Prados, M.; Heideman, R. Phase I
20
21 clinical trial of mafosfamide in infants and children aged 3 years or younger with newly
22
23 diagnosed embryonal tumors: a pediatric brain tumor consortium study. *J. Clin. Oncol.* **2005**, *23*,
24
25 525–531.
26
27
28 (11) Paci, A.; Martens, T.; Royer, J. Anodic oxidation of ifosfamide and cyclophosphamide: a
29
30 biomimetic metabolism model of the oxazaphosphorinane anticancer drugs. *Bioorg. Med. Chem.*
31
32 *Lett.* **2001**, *11*, 1347-1349.
33
34
35 (12) Hohorst, H. J.; Peter, G.; Struck, R. F. Synthesis of 4-hydroperoxy derivatives of ifosfamide
36
37 and trofosfamide by direct ozonation and preliminary antitumor evaluation *in vivo*. *Cancer Res.*
38
39 **1976**, *36*, 2278-2281.
40
41
42 (13) Takamizawa, A.; Matsumoto, S.; Iwata, T.; Makino, I. Synthesis, stereochemistry and
43
44 antitumor activity of 4-hydroperoxyisophosphamide (NSC-227114) and related compounds.
45
46 *Chem. Pharm. Bull.* **1977**, *25*, 1877-1891.
47
48
49 (14) Bockstael, M. 4-Carbamoyloxy-oxazaphosphorines, procédé pour leur fabrication et
50
51 préparations pharmaceutiques contenant celle-ci. *Belgium Patent.* **1982**, *880*, 276.
52
53
54 (15) Couvreur, P. Nano-assemblies in drug delivery: past, present and future. *Adv. Drug Deliv.*
55
56 *Rev.* **2013**, *65(1)*, 21-23.
57
58
59
60

- 1
2
3
4
5 (16) Couvreur, P.; Stella, B.; Reddy, L. H.; Hillaireau, H.; Dubernet, C.; Desmaële, D.; Lepêtre-
6 Mouelhi, S.; Rocco, F.; Dereuddre-Bosquet, N.; Clayette, P.; Rosilio, V.; Marsaud, V.; Renoir,
7 J.-M.; Cattel, L. Squalenoylnanomedicines as potential therapeutics. *Nano Lett.* **2006**, *6*, 2544–
8 2548.
9
10 (17) Couvreur, P.; Reddy, L. H.; Mangenot, S.; Poupaert, J. H.; Desmaële, D.; Lepêtre-Mouelhi,
11 S.; Pili, B.; Bourgaux, C.; Amenitsch, H.; Ollivon, M. Discovery of new hexagonal
12 supramolecular nanostructures formed by squalenylation of an anticancer nucleoside analogue.
13 *Small.* **2008**, *4*, 247–253.
14
15 (18) Desmaële, D.; Gref, G.; Couvreur, P. Squalenylation: a generic platform for nanoparticulate
16 drug delivery. *J. Controlled Release.* **2012**, *161*, 609-618.
17
18 (19) Maksimenko, A. ; Dosio, F. ; Mougín, J. ; Ferreo, A.; Wack, S.; Reddy, L.H.; Weyn, A. A.;
19 Lepeltier, E.; Bourgaux, C.; Stella, B.; Cattel, L.; Couvreur, P. A unique squalenoylated and
20 nonpegylated doxorubicin nanomedicine with systemic long-circulating properties and
21 anticancer activity. *Proc. Natl. Acad. Sci. U.S.A.* **2014**, *111*(2), 217-226.
22
23 (20) Sémiramoth, N.; Di Meo, C.; Zouhiri, F.; Saïd Hassane, F.; Valetti, S.; Gorges, R.; Nicolas,
24 V.; Poupaert, J. H.; Chollet-Martin, S.; Desmaële, D.; Gref, R.; Couvreur, P. Self-assembled
25 squalenoylated penicillin bioconjugates: an original approach for the treatment of intracellular
26 infections. *ACS Nano.* **2012**, *6*, 3820-3831.
27
28 (21) Desmaële, D.; Caron, J.; Maksimenko, A.; Wack, S.; Lepeltier, E.; Bourgaux, C.; Couvreur,
29 P.; Morvan, E.; Leblanc, K. Improving the antitumor activity of squalenoyl-paclitaxel conjugate
30 nano-assemblies by manipulating the linker between paclitaxel and squalene. *Adv. Healthcare*
31 *Mater.* **2013**, *2*, 172-185.
32
33
34
35
36
37
38
39
40
41
42
43
44
45
46
47
48
49
50
51
52
53
54
55
56
57
58
59
60

- 1
2
3
4
5 (22) Maksimenko, A. ; Mougin, J.; Mura, S.; Sliwinski, E.; Lepeltier, E.; Bourgaux, C.; Lepêtre-
6 Mouehli, S.; Zouhiri, F.; Desmaële, D.; Couvreur, P. Poly-isoprenoyl gemcitabine conjugates
7 self assemble as nano-assemblies, useful for cancer therapy. *Cancer Lett.* **2013**, *334*, 346-353.
8
9
10 (23) Van Tamelen, E. E.; Curphey, T. J. The selective *in vitro* oxidation of the terminal double
11 bound in squalene. *Tetrahedron Lett.* **1962**, *3*, 121–124.
12
13 (24) Sen, S.S.; Prestwich, G. D. Trisnorsqualene alcohol, a potent inhibitor of vertebrate
14 squaleneepoxidase. *J. Am. Chem. Soc.* **1989**, *111*, 1508–1510.
15
16 (25) Masurel, D.; Houghton P.J.; Young, C.L.; Wainer, I.W. Efficacy, toxicity, pharmacokinetics,
17 and *in vitro* metabolism of the enantiomers of ifosfamide in mice. *Cancer Res.* **1990**, *50*, 252.
18
19 (26) Oliveira RV, Onorato JM, Siluk D, Walko CM, Lindley C, Wainer IW. Enantioselective
20 liquid chromatography-mass spectrometry assay for the determination of ifosfamide and
21 identification of the N-dechloroethylated metabolites of ifosfamide in human plasma. *J Pharm*
22 *Biomed Anal.* **2007**; *45(2)*, 295-303.
23
24 (27) Toulmé, F.; Le Cam, E.; Teyssier, C.; Delain, E.; Sautière, P.; Maurizot, J.C.; Culard, F.
25 Conformational changes of DNA minicircles upon the binding of the archaeobacterial histone-
26 like protein MC1. *J. Biol. Chem.* **1995**, *270 (11)*, 6286-6291.
27
28 (28) Sadagopan, N.; Cohen, L.; Roberts, B.; Collard, W.; Omer, C. Liquid chromatography-
29 tandem mass spectrometric quantitation of cyclophosphamide and its hydroxy metabolite in
30 plasma and tissue for determination of tissue distribution. *J. Chromatogr. B. Biomed. Appl.* **2001**,
31 *759*, 277-284.
32
33 (29) Kerbusch, T.; Huitema, A. D.; Kettenes-van den Bosch, J. J.; Keizer, H. J.; Ouwerkerk, J.; de
34 Kraker, J.; Beijnen, J. H. High-performance liquid chromatographic determination of stabilized 4-
35
36
37
38
39
40
41
42
43
44
45
46
47
48
49
50
51
52
53
54
55
56
57
58
59
60

1
2
3
4
5 hydroxyifosfamide in human plasma and erythrocytes. *J. Chromatogr. B. Biomed. Sci. Appl.*
6
7
8 **1998**, 716, 275-284.
9
10
11
12
13
14
15
16
17
18
19
20
21
22
23
24
25
26
27
28
29
30
31
32
33
34
35
36
37
38
39
40
41
42
43
44
45
46
47
48
49
50
51
52
53
54
55
56
57
58
59
60

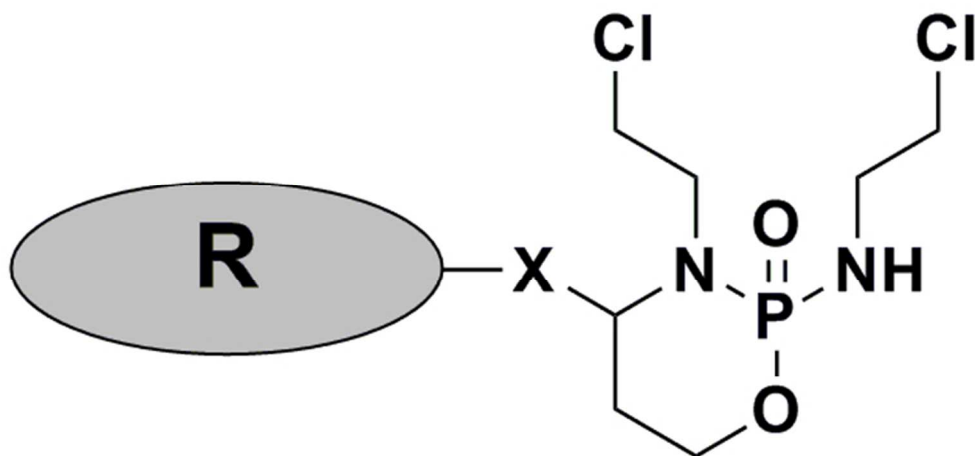
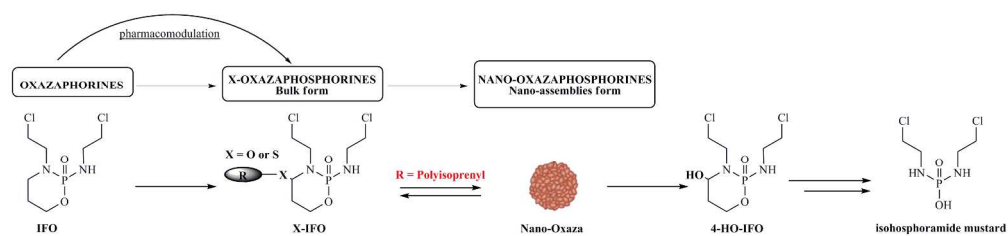
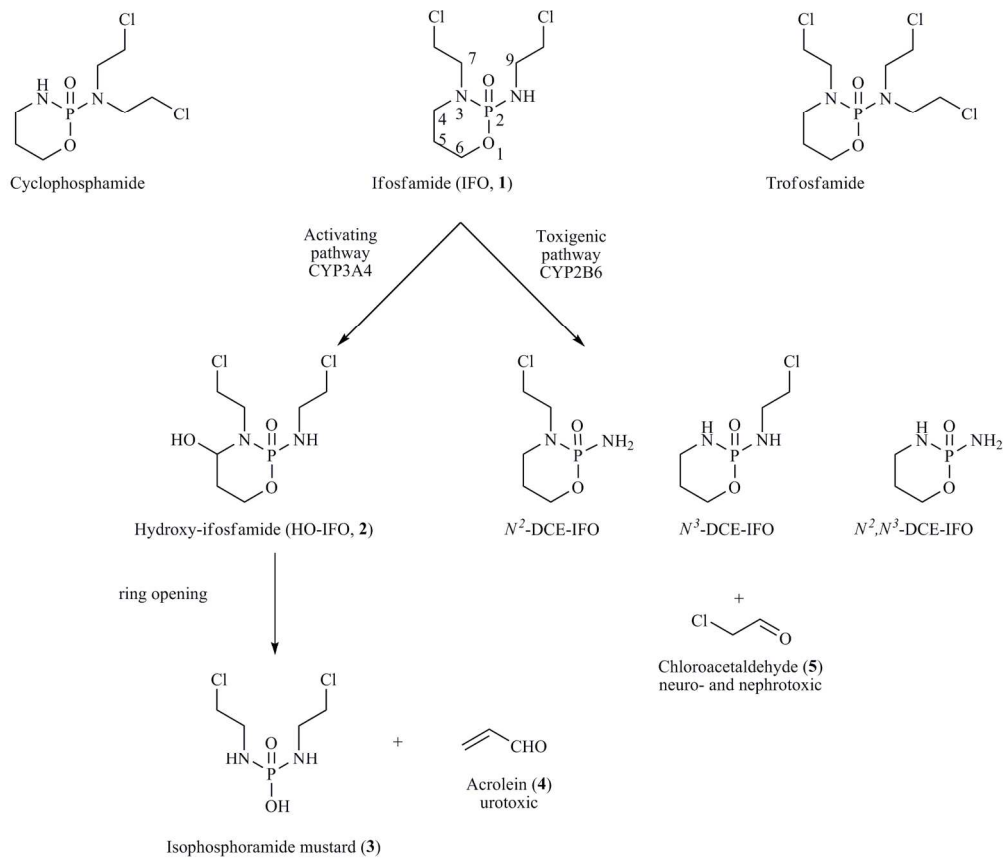


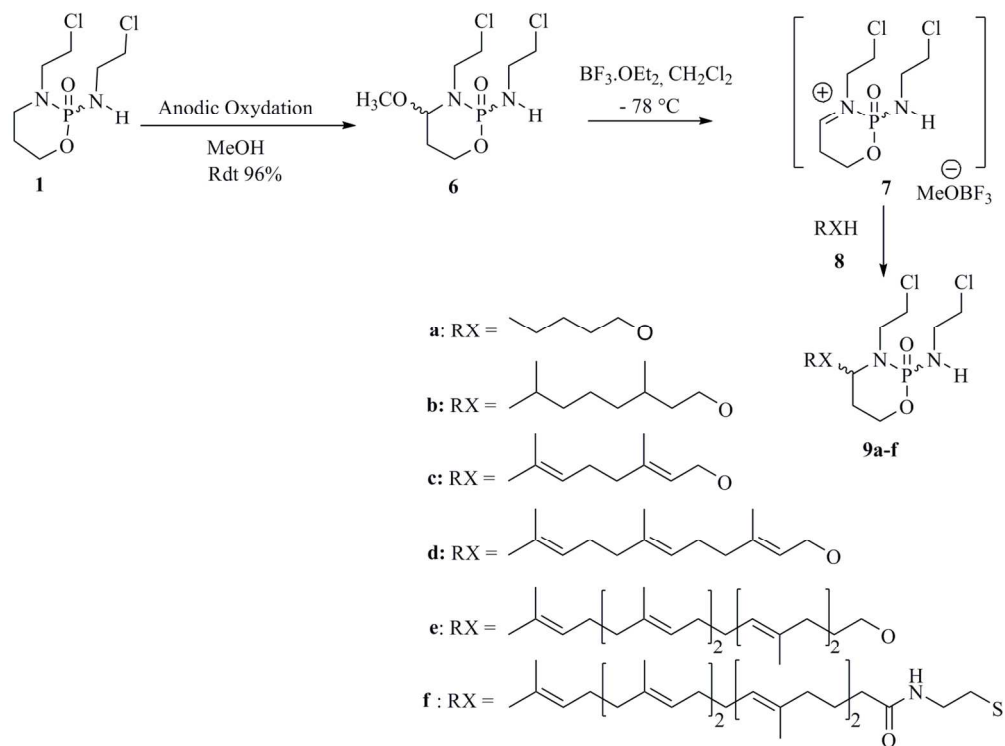
Figure in Abstract
54x26mm (300 x 300 DPI)



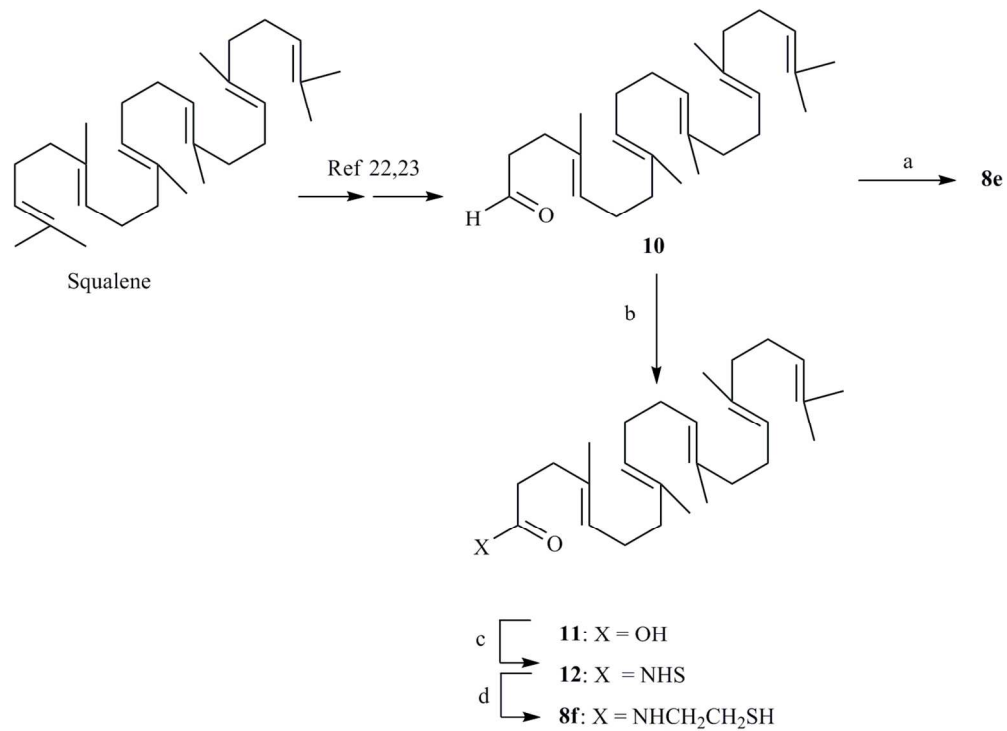
239x54mm (300 x 300 DPI)



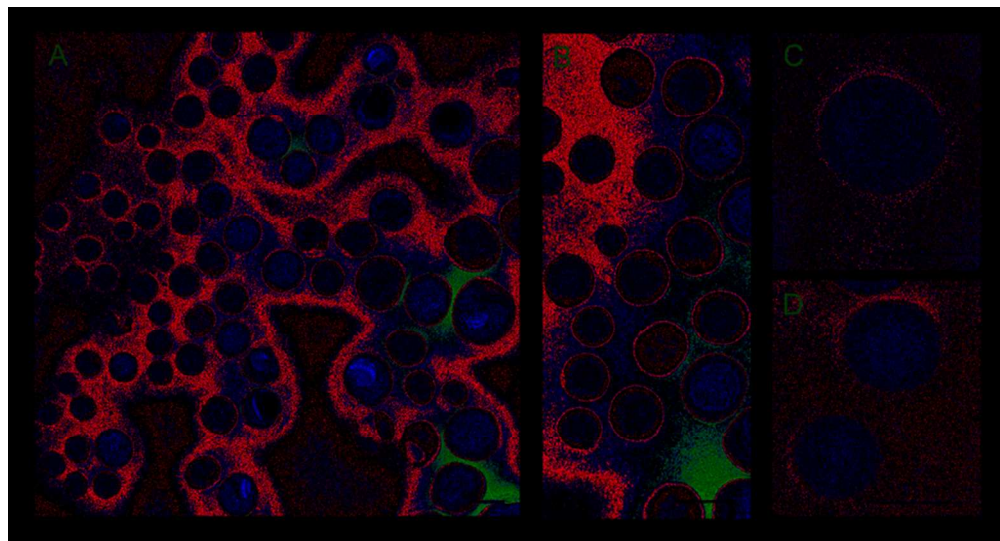
161x137mm (300 x 300 DPI)



134x100mm (300 x 300 DPI)

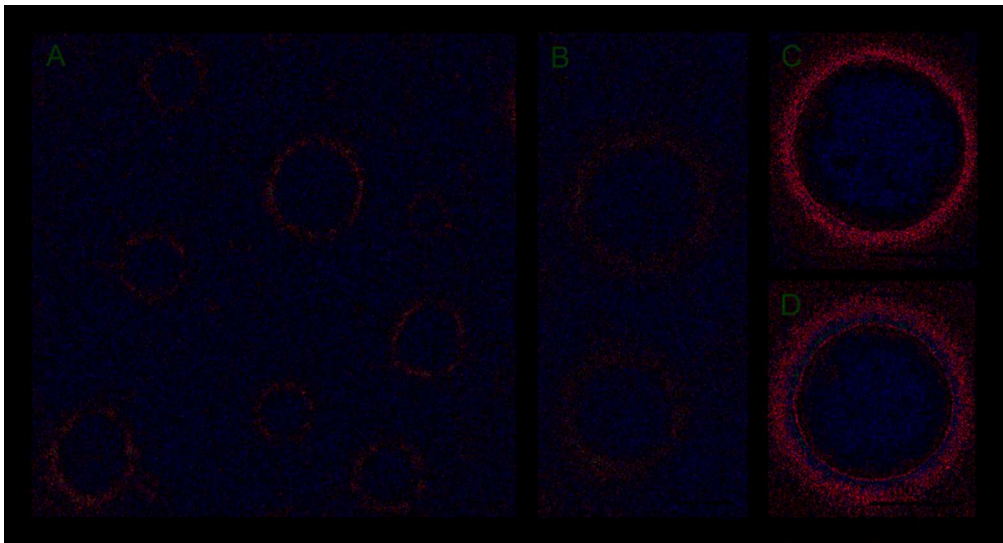


123x90mm (300 x 300 DPI)

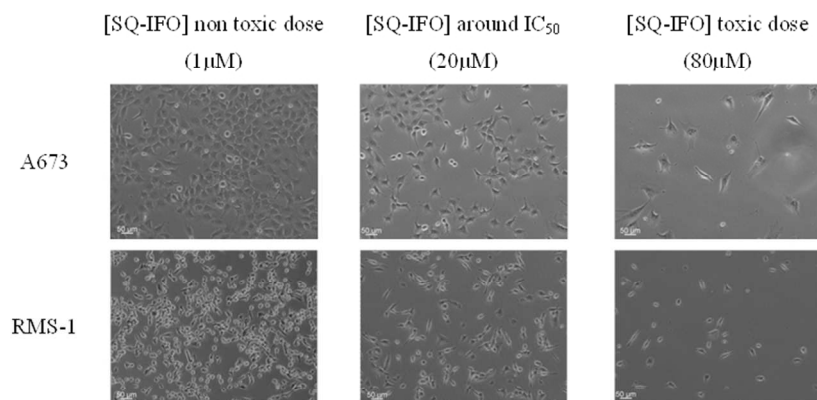


77x41mm (300 x 300 DPI)

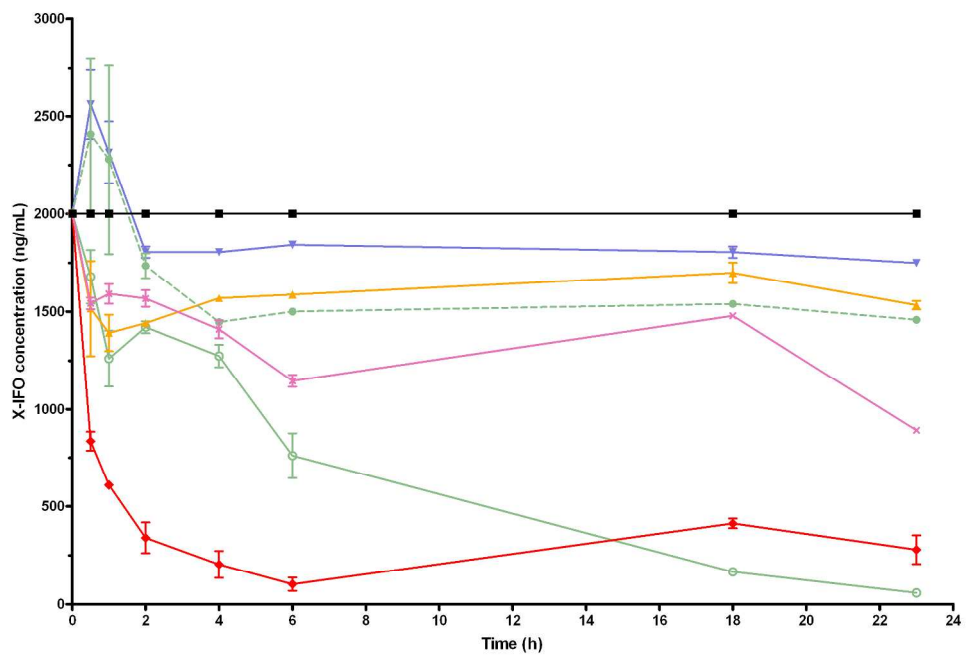
1
2
3
4
5
6
7
8
9
10
11
12
13
14
15
16
17
18
19
20
21
22
23
24
25
26
27
28
29
30
31
32
33
34
35
36
37
38
39
40
41
42
43
44
45
46
47
48
49
50
51
52
53
54
55
56
57
58
59
60



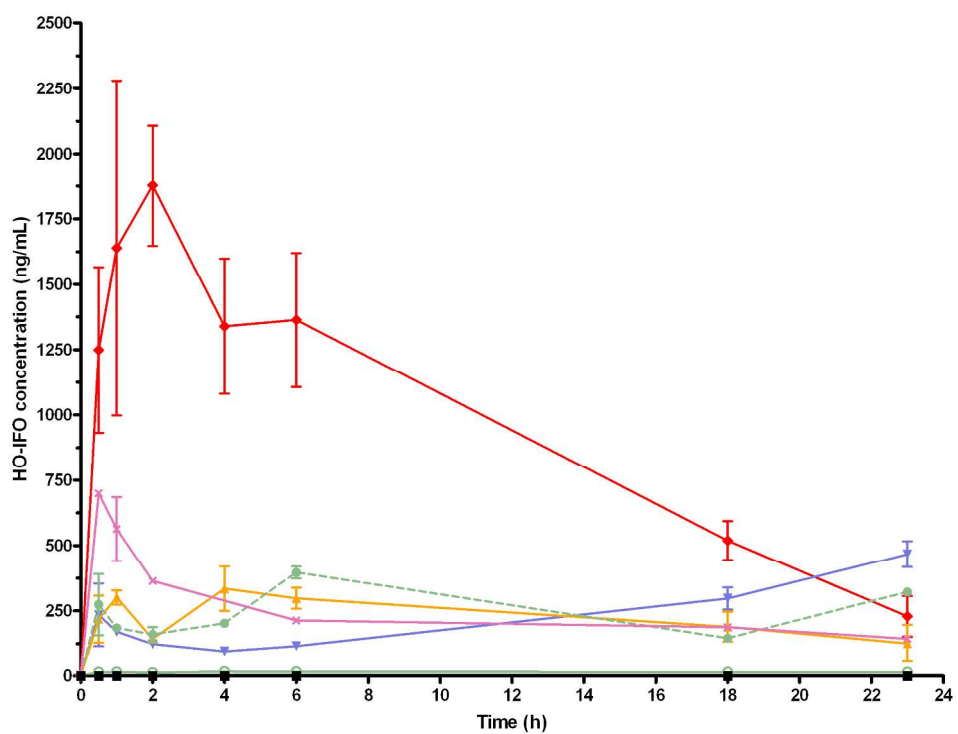
78x42mm (300 x 300 DPI)



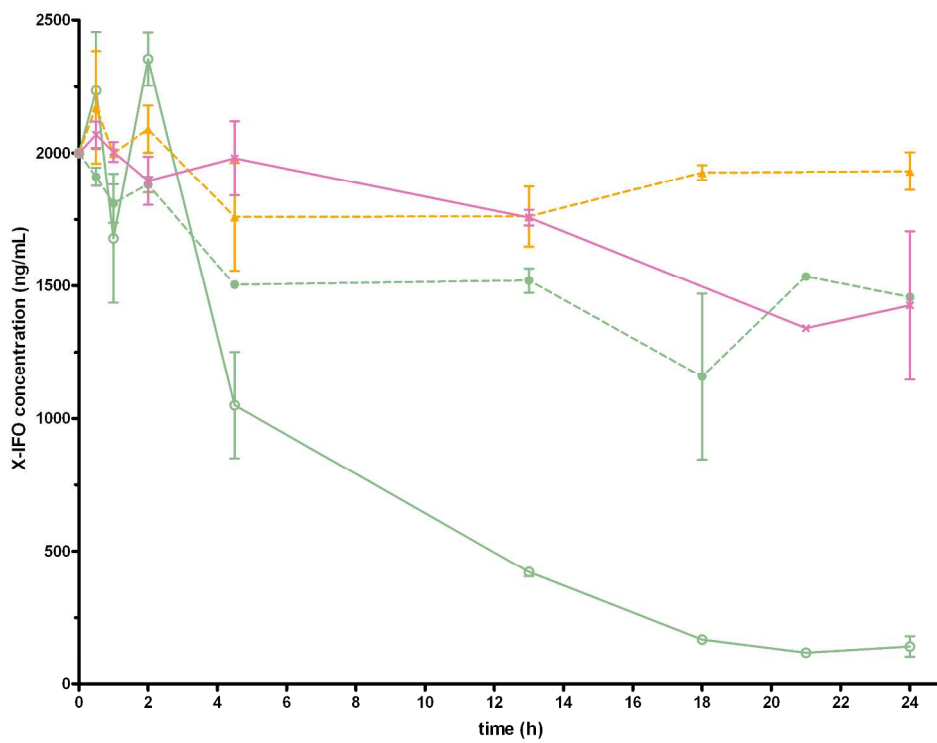
254x190mm (96 x 96 DPI)



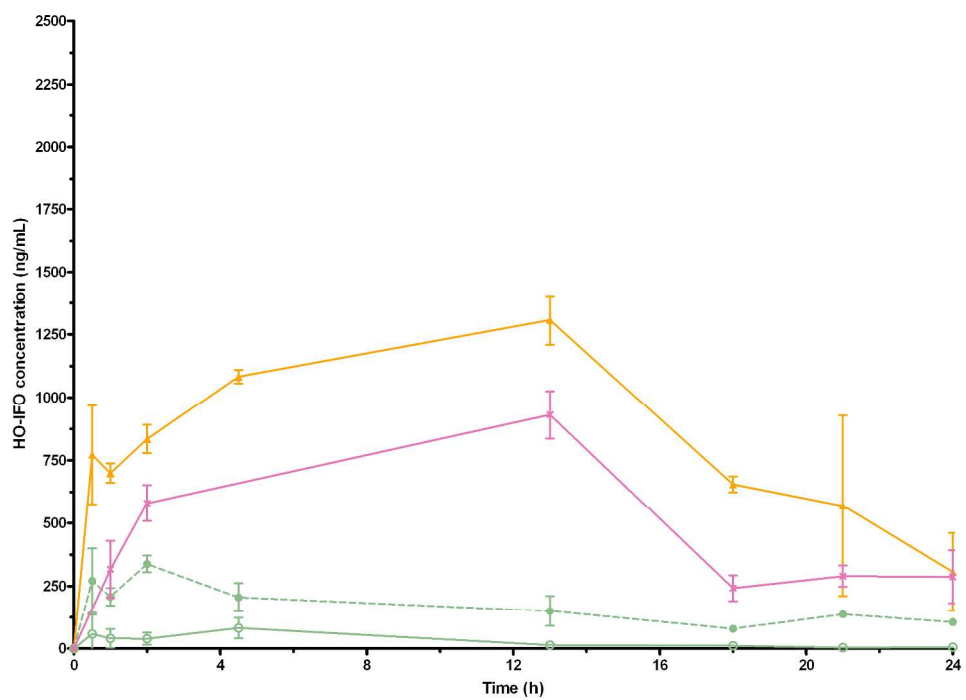
262x177mm (300 x 300 DPI)



227x172mm (300 x 300 DPI)



232x178mm (300 x 300 DPI)



260x187mm (300 x 300 DPI)